

A sunset scene over a calm body of water. The sun is a bright white circle on the horizon, casting a shimmering orange and red reflection on the water's surface. The sky transitions from a pale blue at the top to a deep orange near the horizon. In the foreground, the dark silhouettes of rocky islands or cliffs are visible against the bright sky.

Recent Progress and Future Directions for Helioseismology

A.G. Kosovichev (Stanford University)

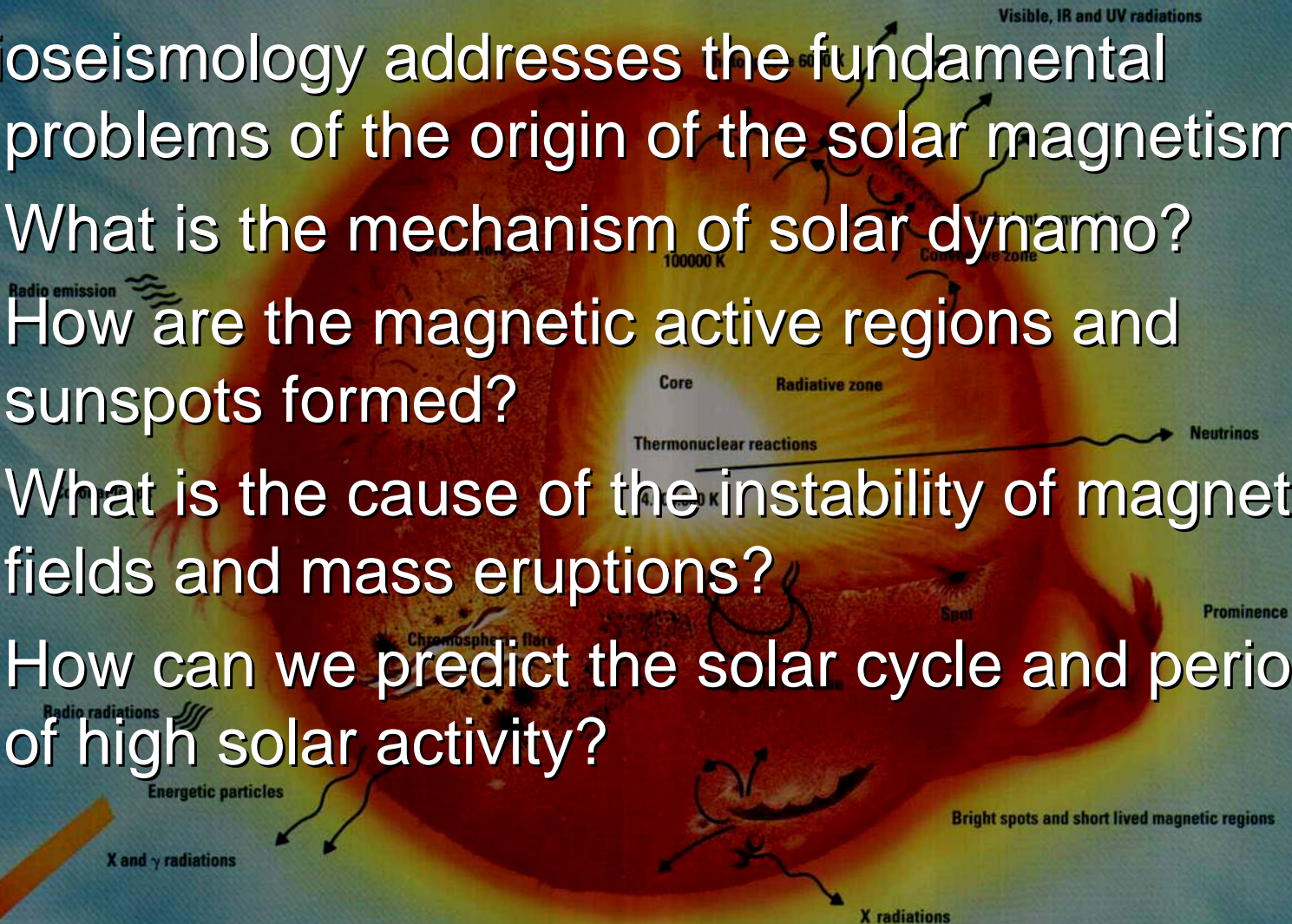
Outline

- Acoustic tomography of the solar dynamics
- Structure and dynamics of sunspots
- MHD waves in sunspots
- Tomographic imaging of the tachocline
- First helioseismology results from Hinode
- Hinode observations of MHD waves excited by a solar flare
- Solar Dynamics Observatory (SDO) and other space projects

Basic questions of helioseismology

Helioseismology addresses the fundamental problems of the origin of the solar magnetism:

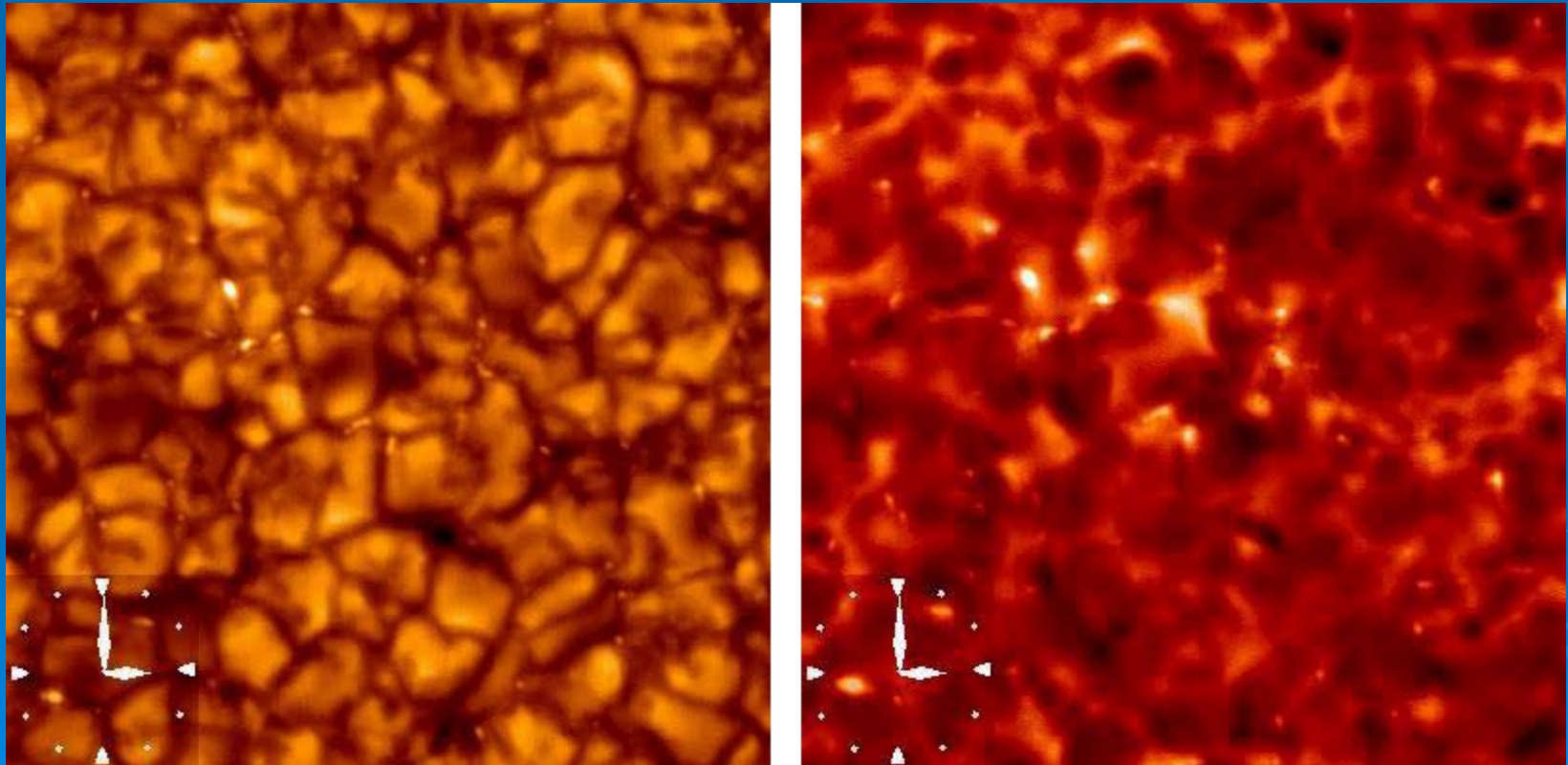
- What is the mechanism of solar dynamo?
- How are the magnetic active regions and sunspots formed?
- What is the cause of the instability of magnetic fields and mass eruptions?
- How can we predict the solar cycle and periods of high solar activity?



Observations of solar oscillations from Hinode

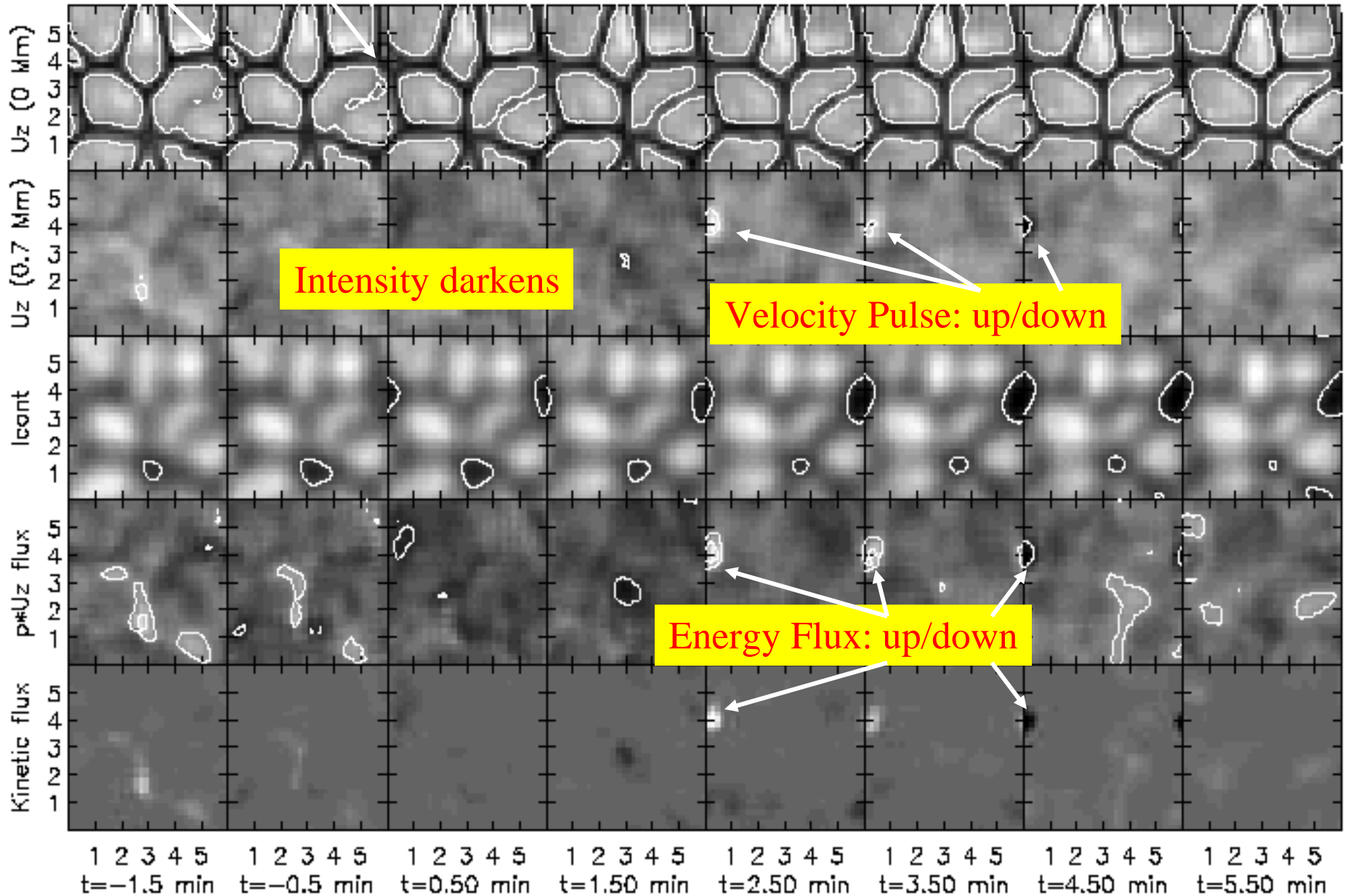
G-band - photosphere

Call H – low chromosphere



Granule disappears

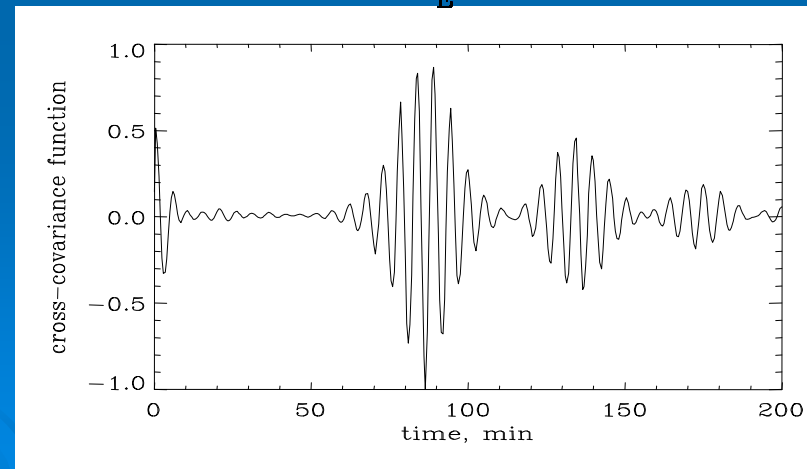
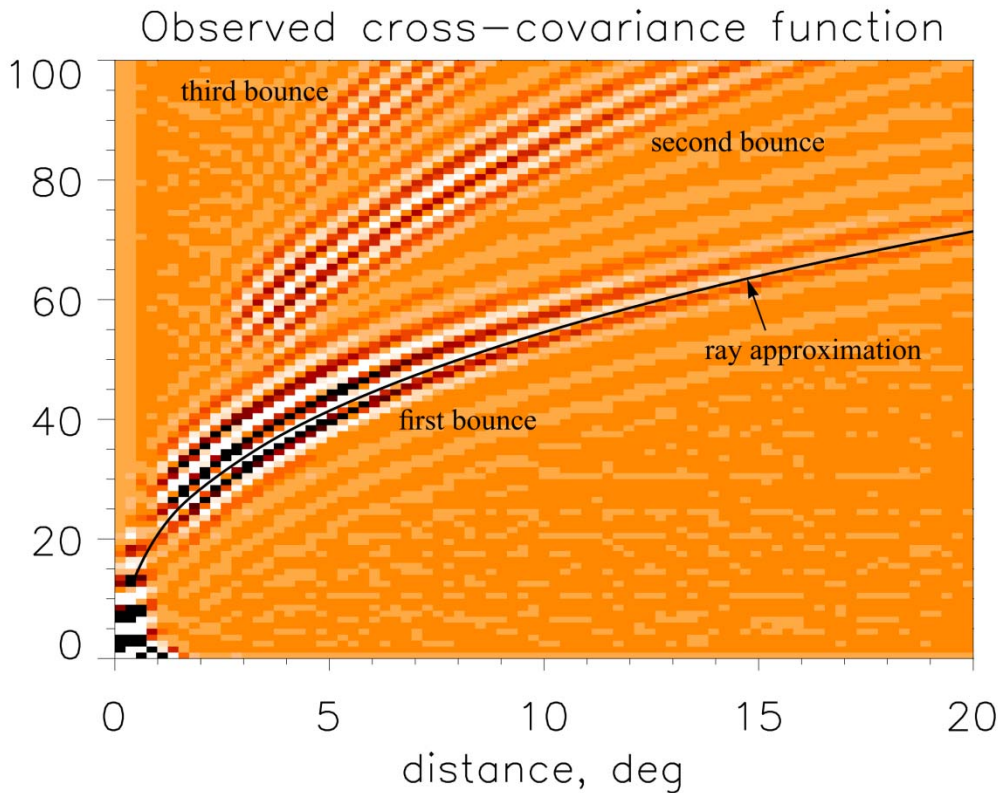
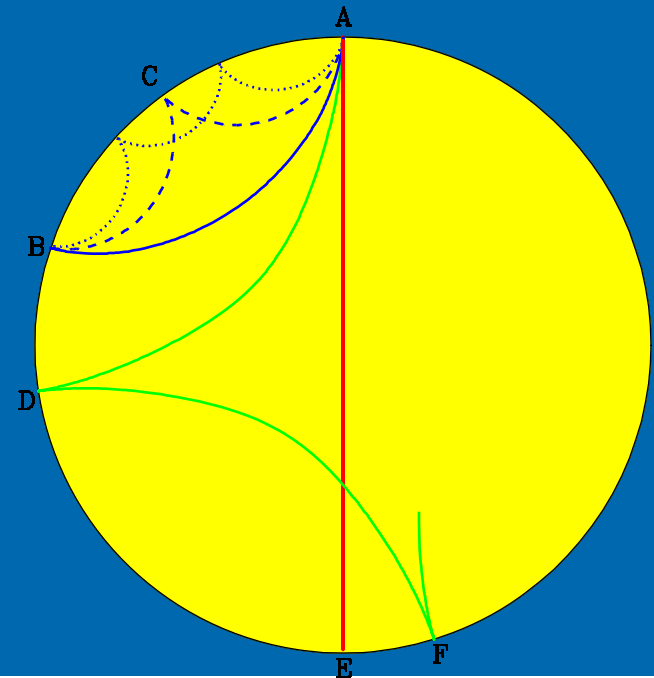
Excitation sources are stochastic: rapid downdrafts in dark intergranular lanes



Time-distance measurements

Travel times are determined from the cross-covariance function (Duvall et al, 1993):

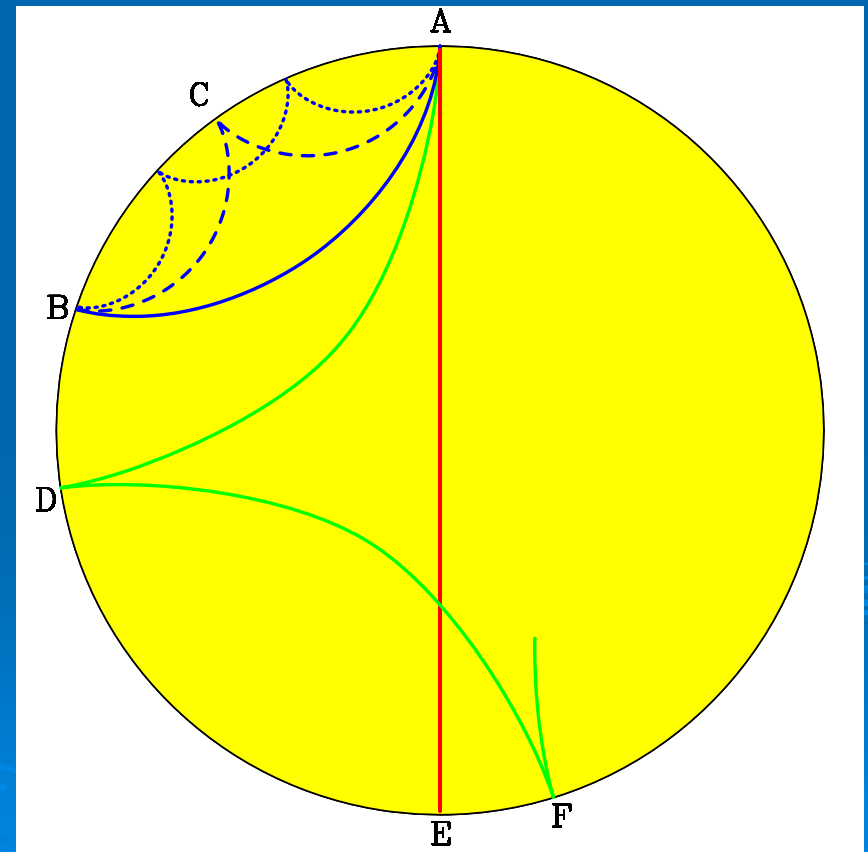
$$\Psi(\tau, \Delta) = \int_0^T f(t, r) f^*(t + \tau, r + \Delta) dt$$



Time-distance helioseismology

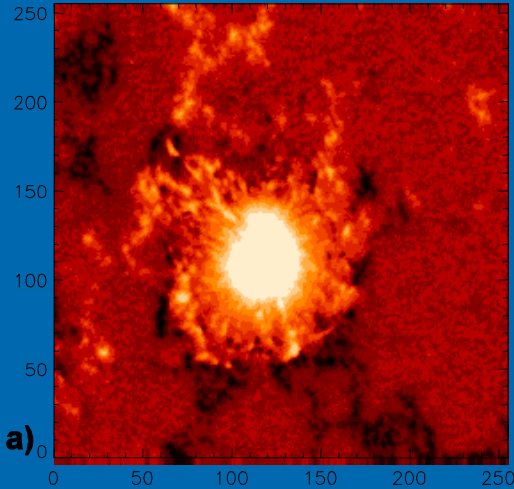
Measures travel times of acoustic or surface gravity waves propagating between different surface points through the interior. The travel times depend on conditions, flow velocity and wave speed along the ray path:

$$\delta\tau = -\int_{\Gamma} \frac{k}{\omega} \frac{\delta w}{c} ds - \int_{\Gamma} \frac{(\vec{n} \cdot \vec{U})}{c^2} ds$$

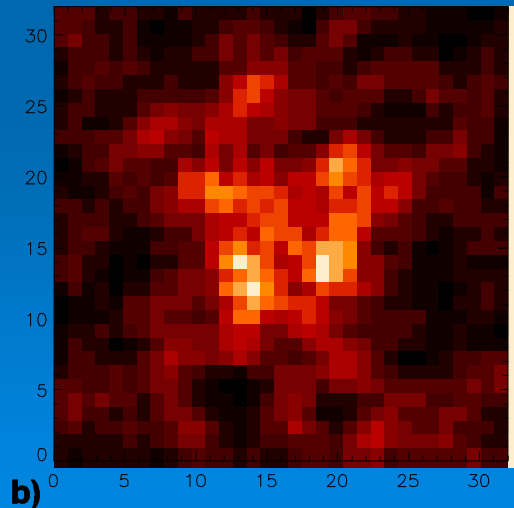


Diagnostics of magnetic field (Zhao & Kosovichev, 2000)

MDI magnetogram



Travel-time anisotropy, A

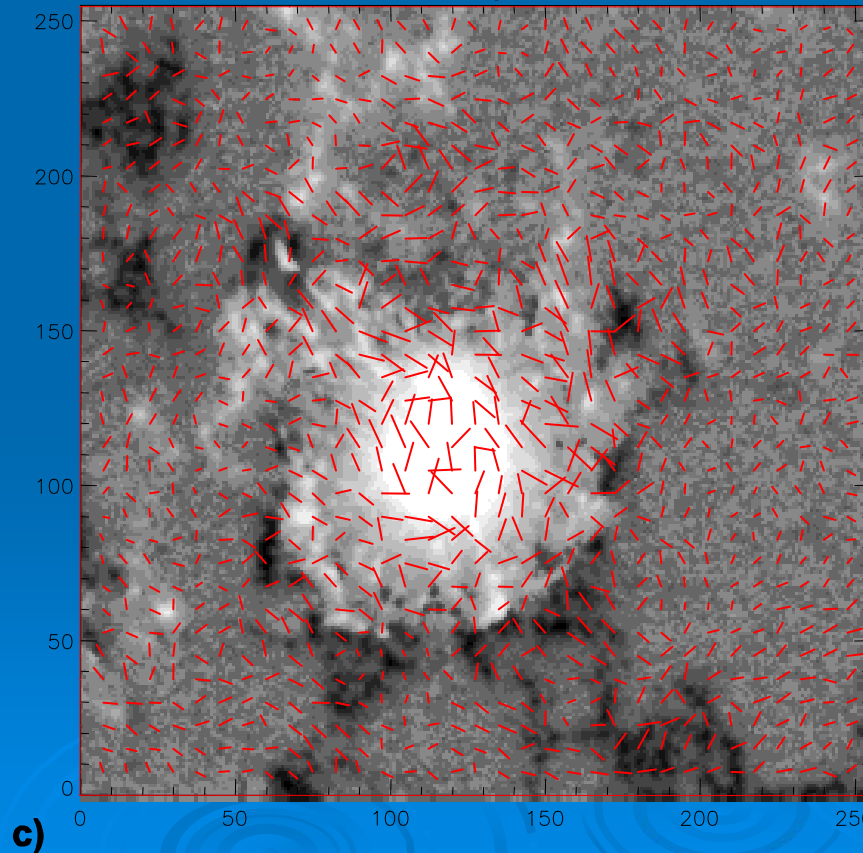


10/20/2008

$$\delta\tau_i = -\int_{\Gamma_i} \left[\frac{(\mathbf{n}\mathbf{U})}{c^2} + \frac{\delta c}{c} S + \left(\frac{\delta\omega_c}{\omega_c} \right) \frac{\omega_c^2}{\omega^2 c^2 S} + \frac{1}{2} \left(\frac{c_A^2}{c^2} - \frac{(\mathbf{k}\mathbf{c}_A)^2}{k^2 c^2} \right) S \right] ds,$$



Horizontal Magnetic Field

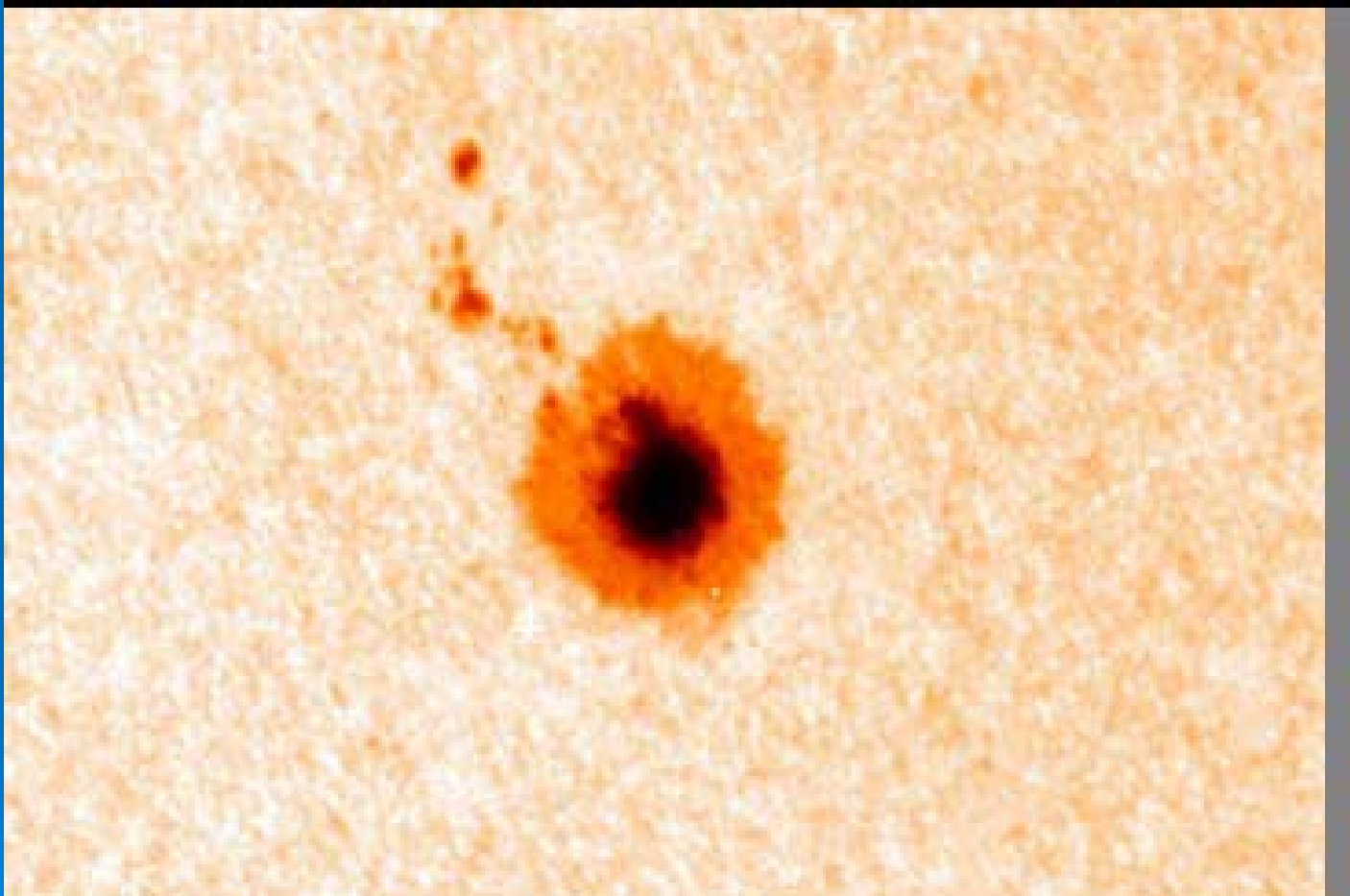


Alfven speed

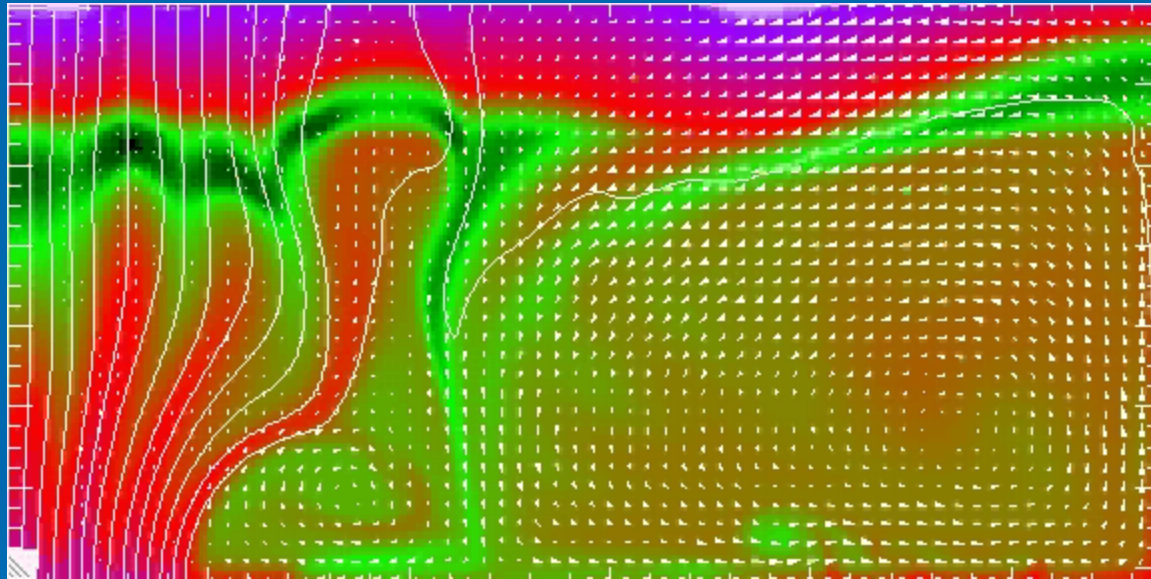
$$c_A = B / \sqrt{4\pi\rho}$$

can
be measured
from
anizotropy of
travel-times.

Sunspot structure and dynamics



Numerical simulations (N.Hurlburt et al, 2008)

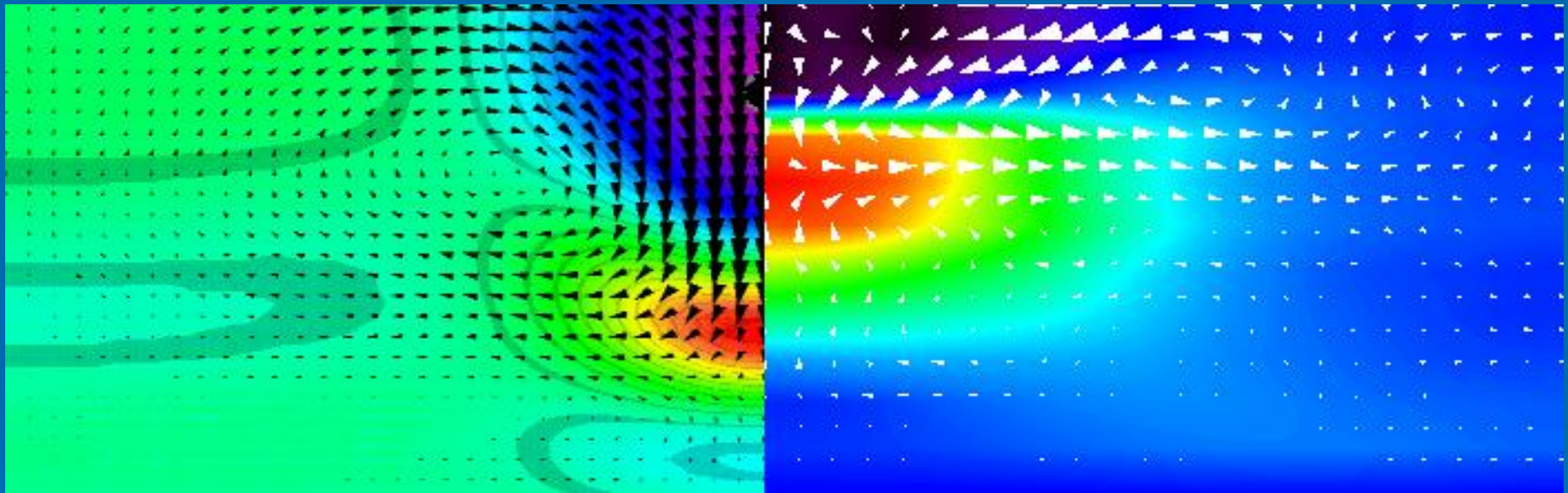


Numerical model of sunspot vs observations

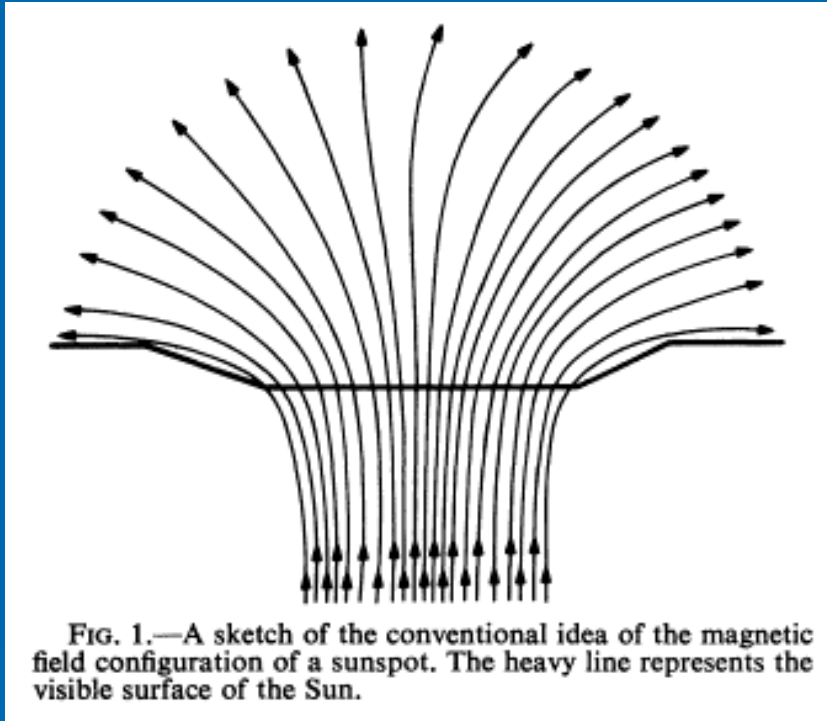
Model

Hurlburt and Rucklidge(2000)

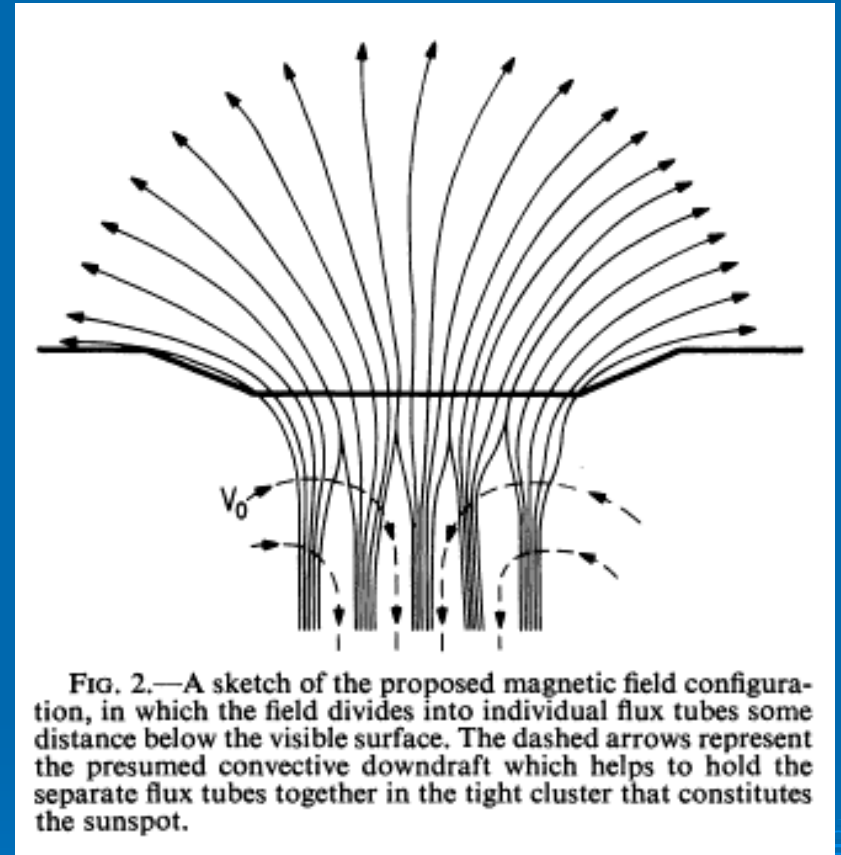
Observations



Parker's model



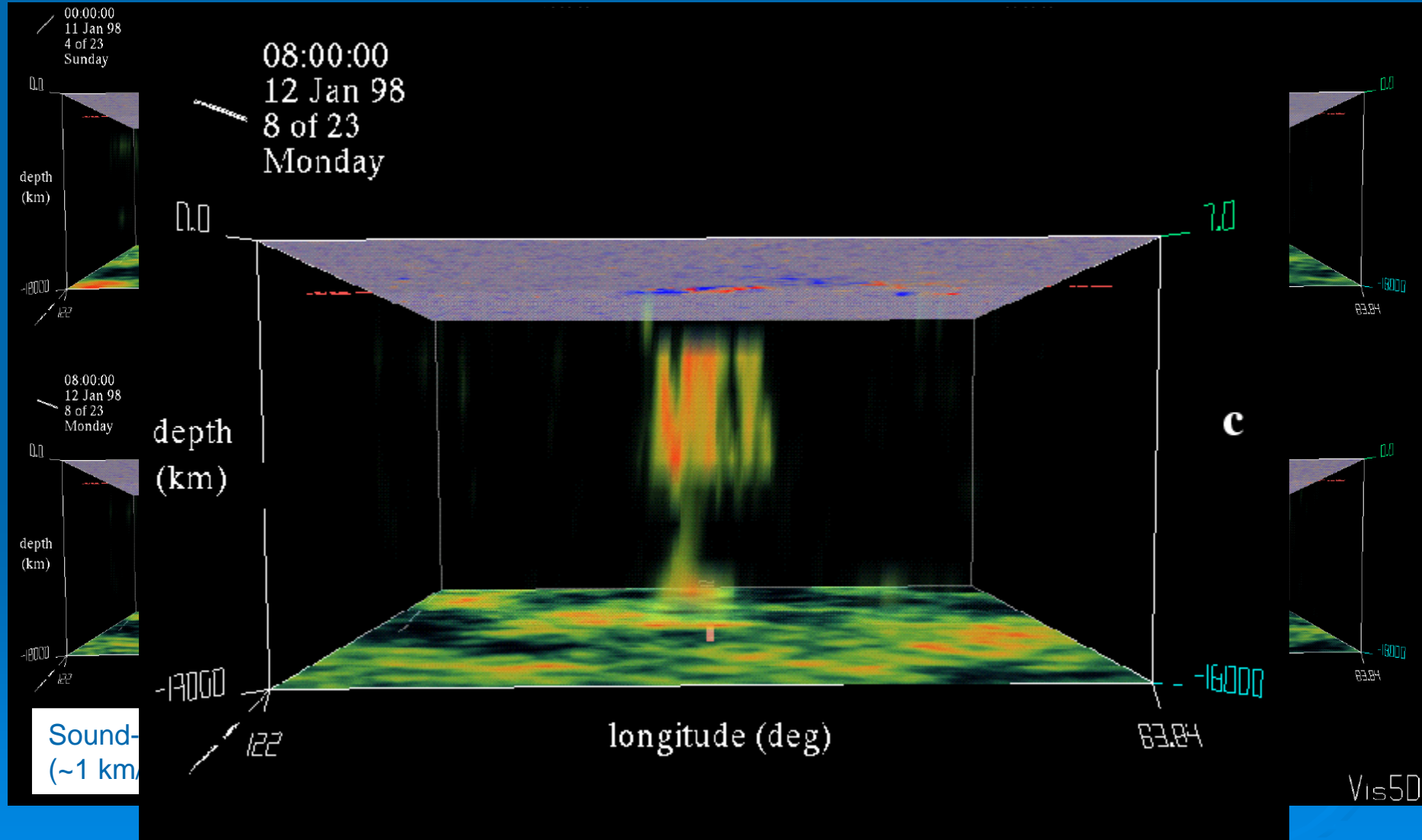
Monolithic model



Cluster Model

Helioseismology observations favor the cluster model

Observations of emerging active region by time-distance helioseismology



Using 3D MHD modeling for verification and testing

$$\frac{\partial \rho'}{\partial t} + \nabla \cdot \mathbf{m}' = 0$$

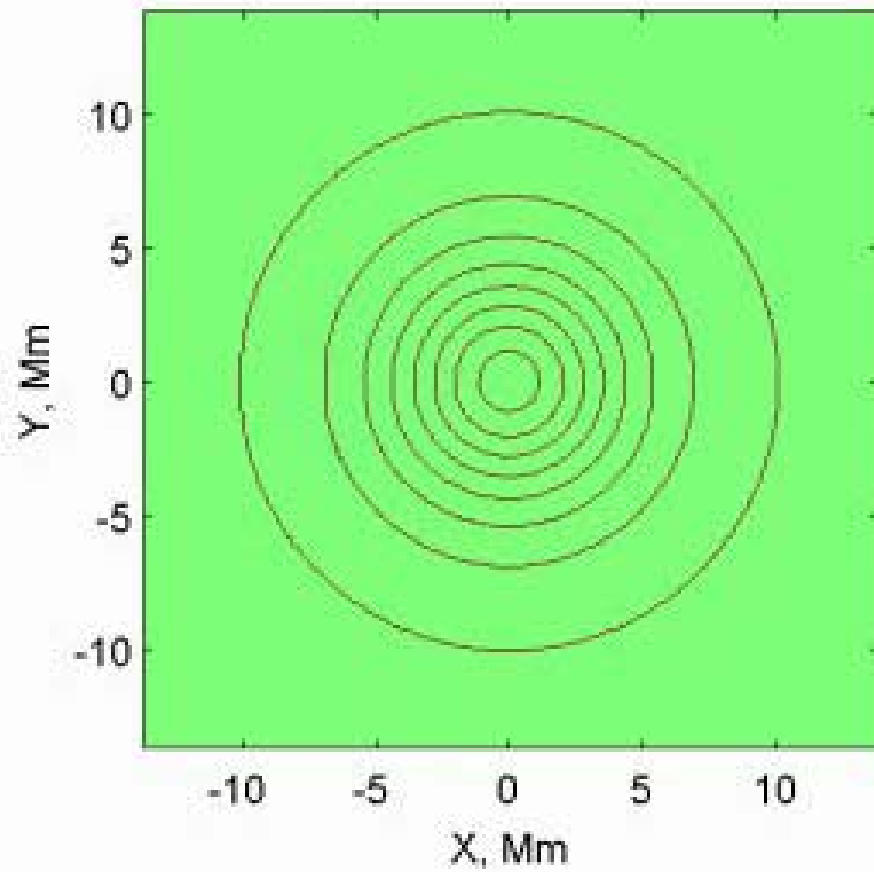
$$\frac{\partial \mathbf{m}'}{\partial t} + \nabla p' - \frac{1}{4\pi} [(\nabla \times \mathbf{B}_0) \times \mathbf{B}' + (\nabla \times \mathbf{B}') \times \mathbf{B}_0] = \rho' \mathbf{g}_0 + \mathbf{S}$$

$$\frac{\partial \mathbf{B}'}{\partial t} = \nabla \times \left(\frac{\mathbf{m}'}{\rho_0} \times \mathbf{B}_0 \right)$$

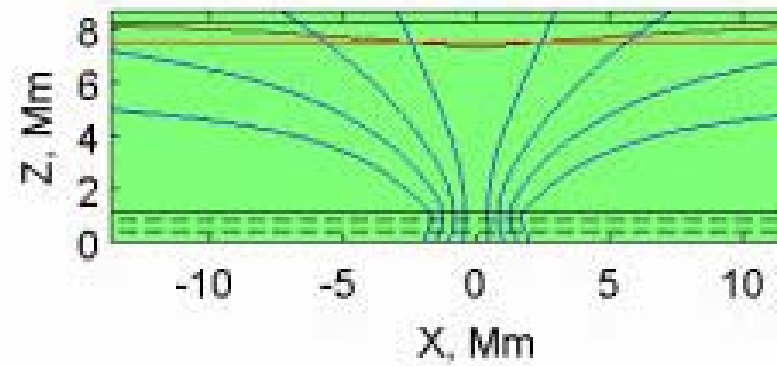
$$\frac{\partial p'}{\partial t} + c_s^2 \left[\nabla \cdot \mathbf{m}' + \mathbf{m}' \cdot \left(\frac{\nabla p_0}{\Gamma_1 p_0} - \frac{\nabla \rho_0}{\rho_0} \right) \right] = 0$$

- Khomenko, E., Kosovichev, A., Collados, M., Parchevsky, K., Olshevsky, V. 2008. Theoretical modeling of propagation of magneto-acoustic waves in magnetic regions below sunspots. ArXiv e-prints arXiv:0809.0278.
- Parchevsky, K.V., Kosovichev, A.G. 2008. Numerical simulation of excitation and propagation of helioseismic MHD waves: Effects of inclined magnetic field. ArXiv e-prints arXiv:0806.2897
- Parchevsky, K.V., Zhao, J., Kosovichev, A.G. 2008. Influence of Nonuniform Distribution of Acoustic Wavefield Strength on Time-Distance Helioseismology Measurements. ApJ 678, 1498-1504
- Parchevsky, K.V., Kosovichev, A.G. 2007. Effect of Suppressed Excitation on the Amplitude Distribution of 5 Minute Oscillations in Sunspots. ApJL 666, L53-L56
- Parchevsky, K.V., Kosovichev, A.~G. 2007. Three-dimensional Numerical Simulations of the Acoustic Wave Field in the Upper Convection Zone of the Sun. ApJ 666, 547-558.

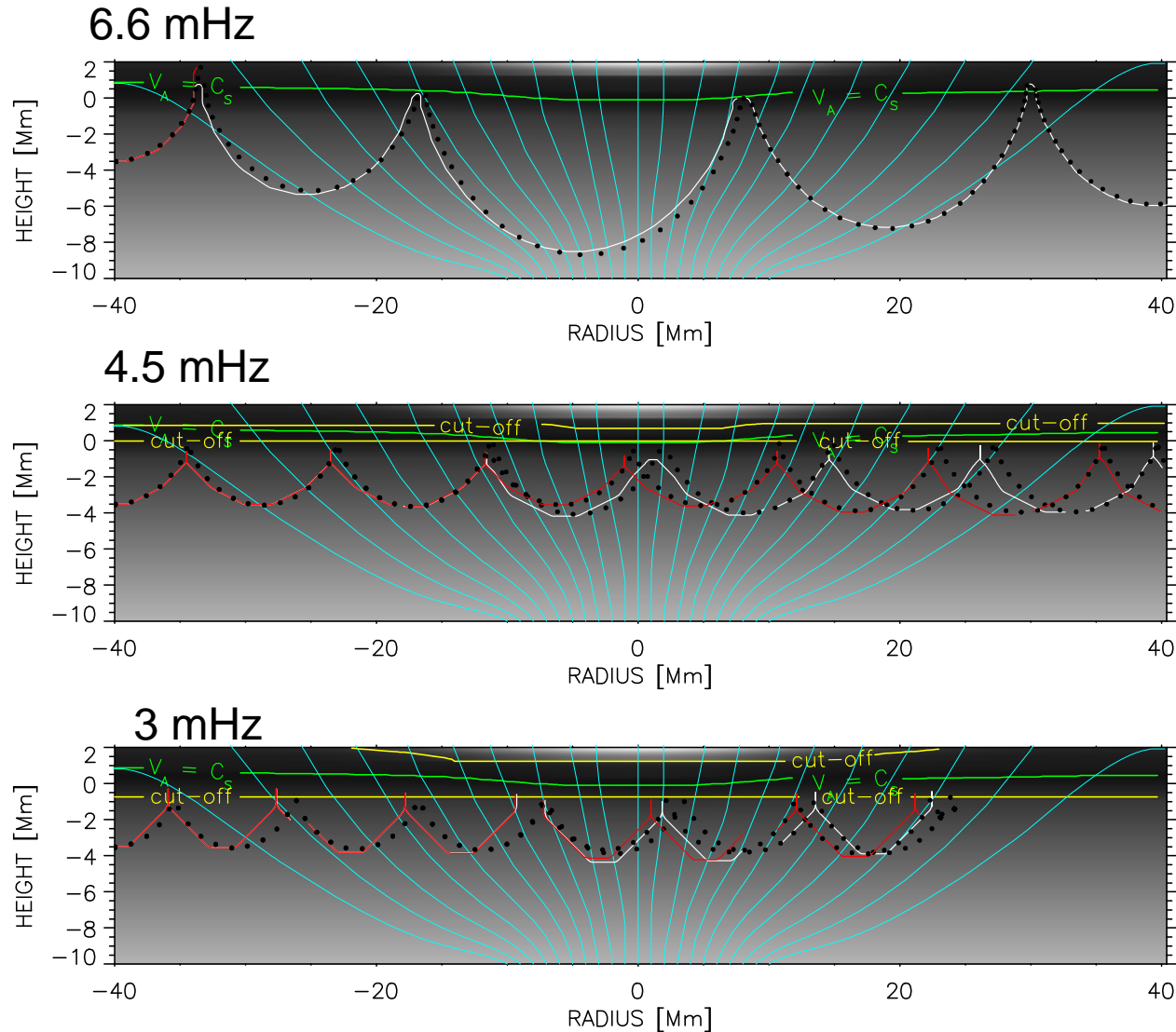
$\rho_0 w$, Depth = 0 Mm



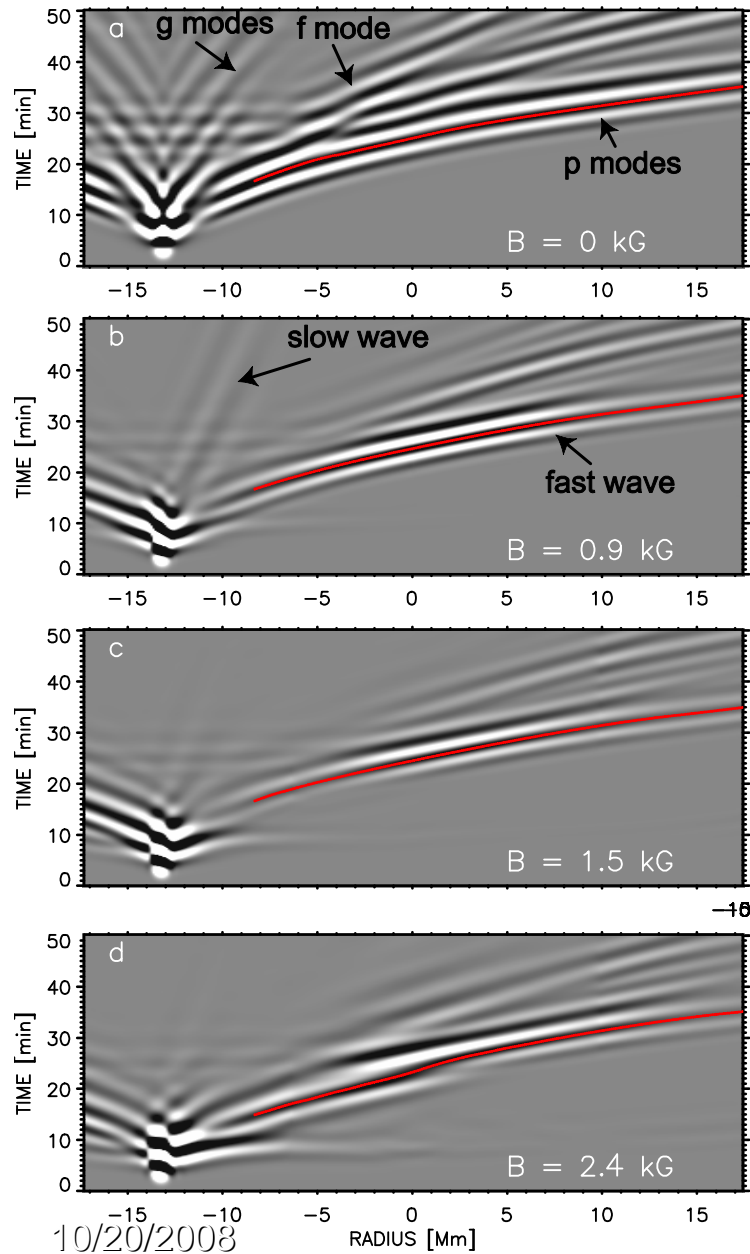
$T_{\text{step}} = 000060$, $t = 0.0500$ min.



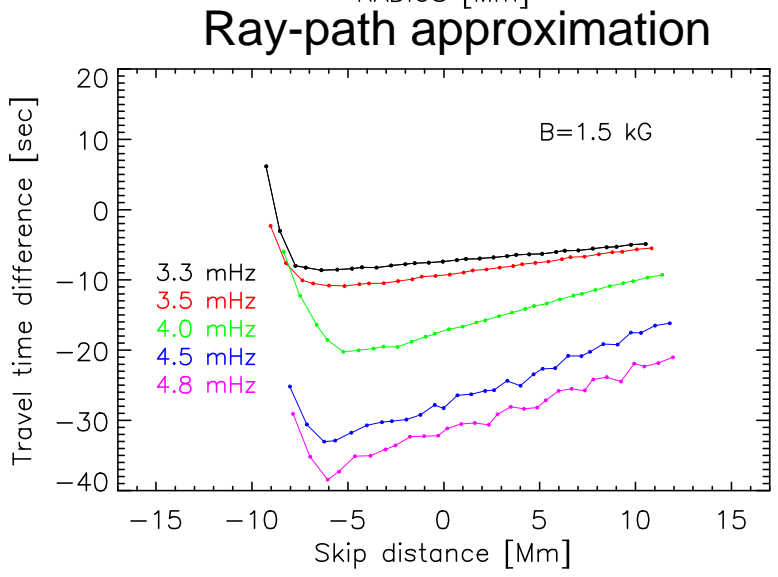
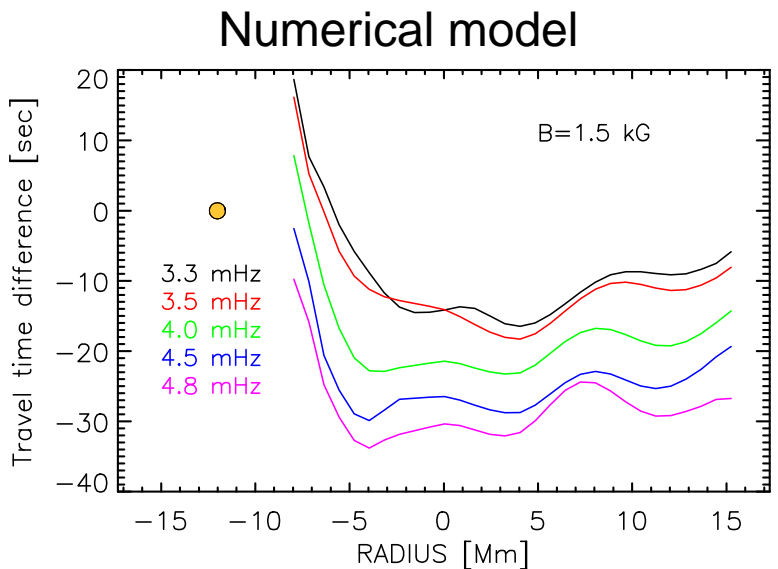
Ray paths calculated in eikonal approximation for $B=2.4$ kG



Time-distance diagram of MHD waves in the sunspot model

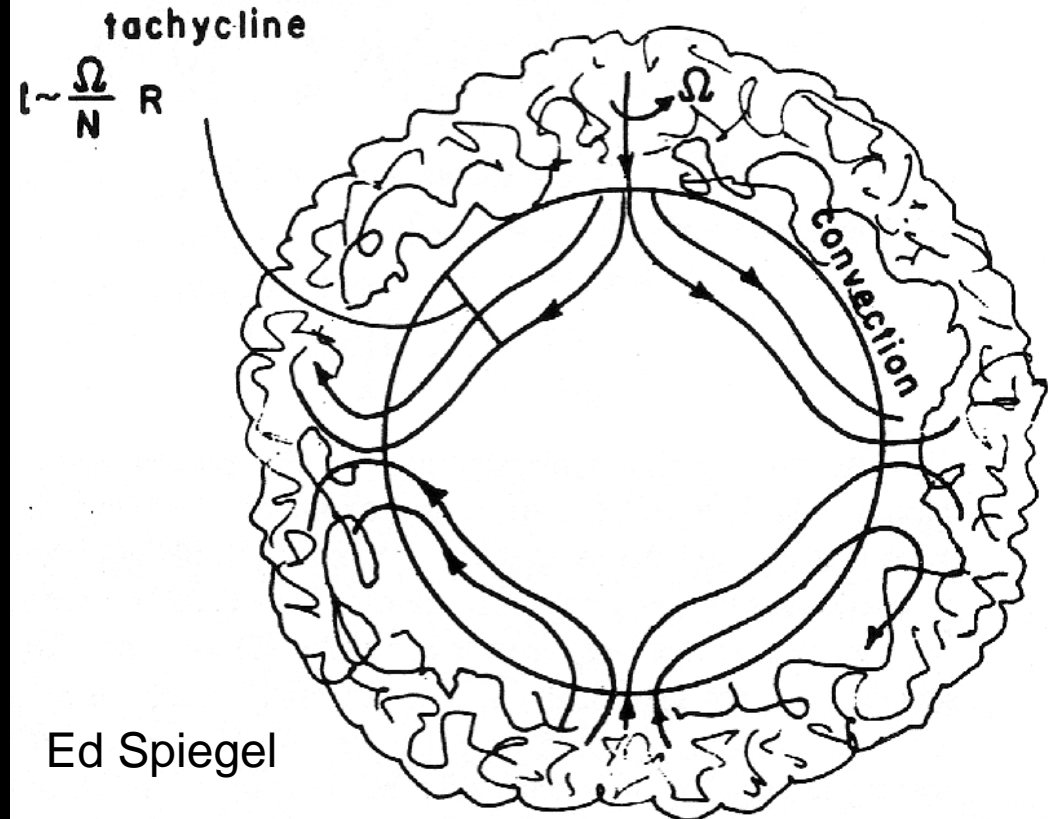
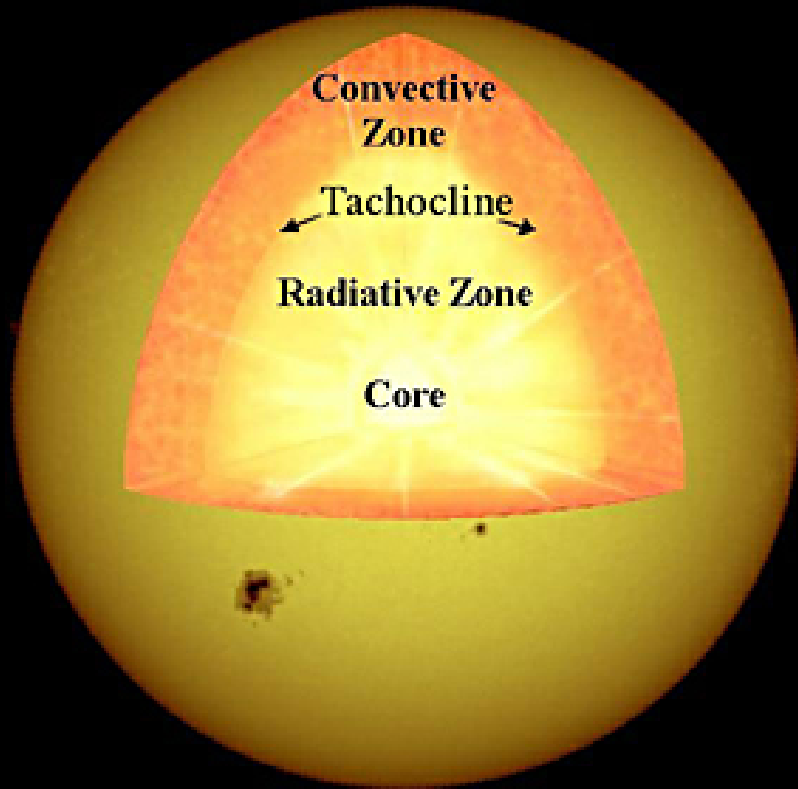


Travel times at different frequencies

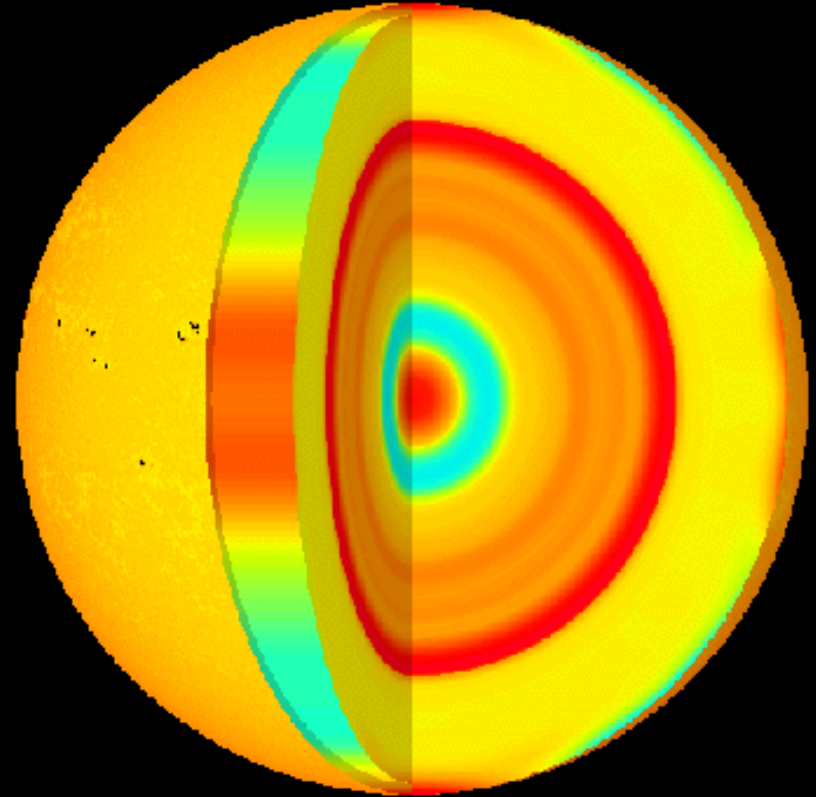
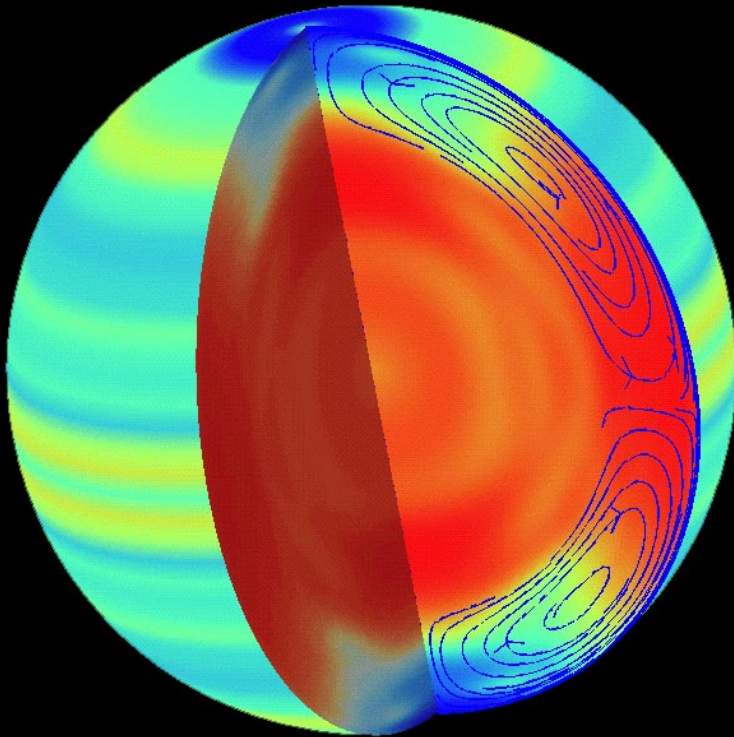


The numerical MHD wave modeling supports the helioseismology procedure and results.

Acoustic Tomography of the Tachocline

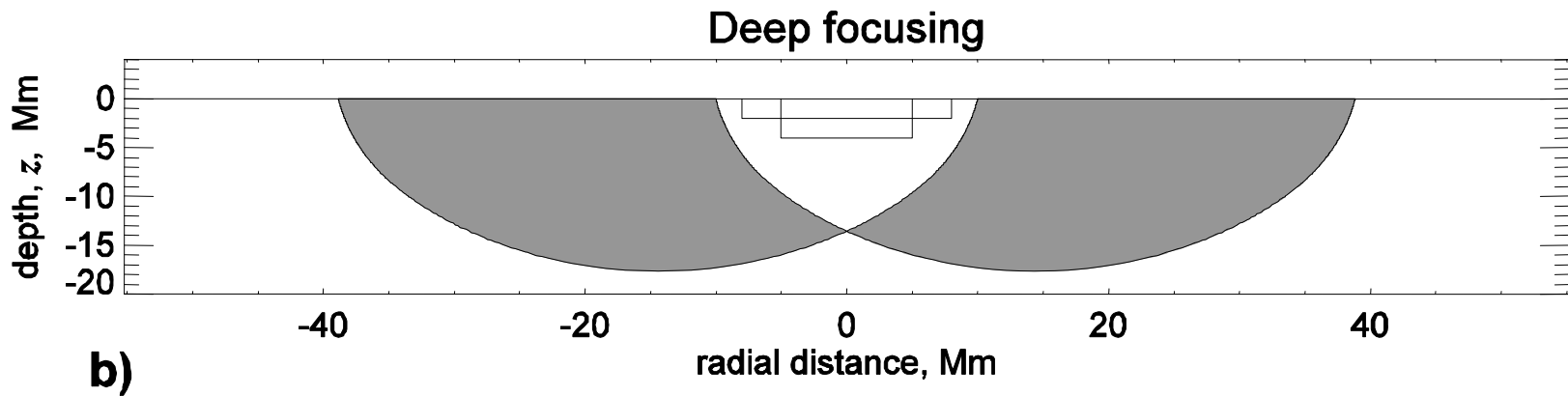
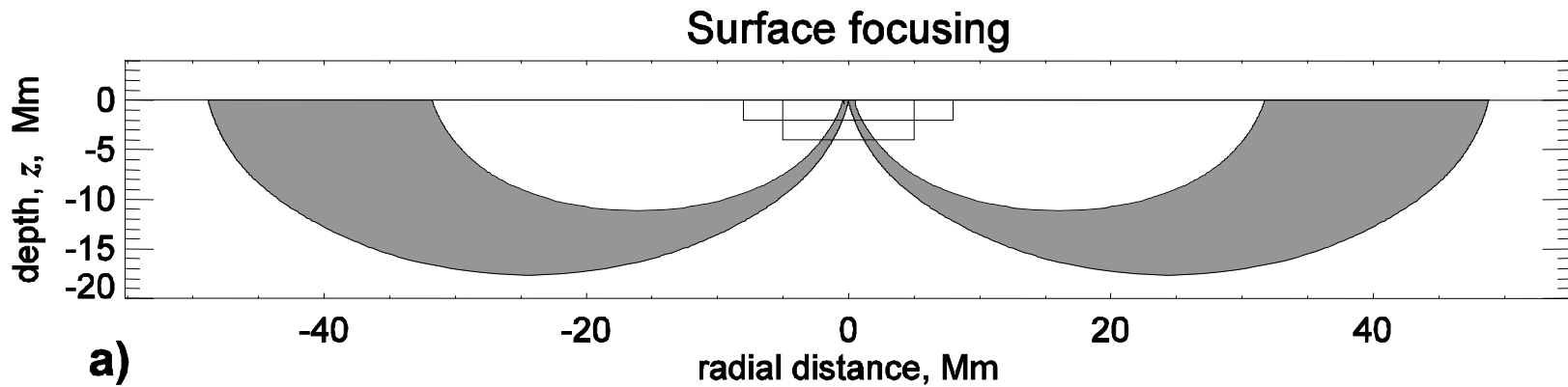


Global helioseismology results

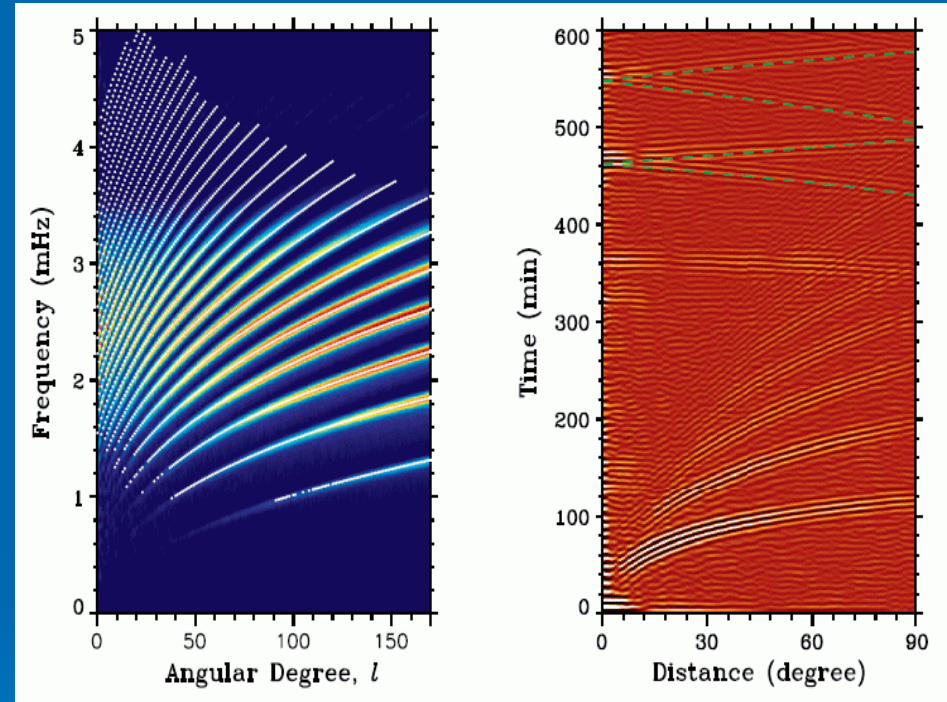
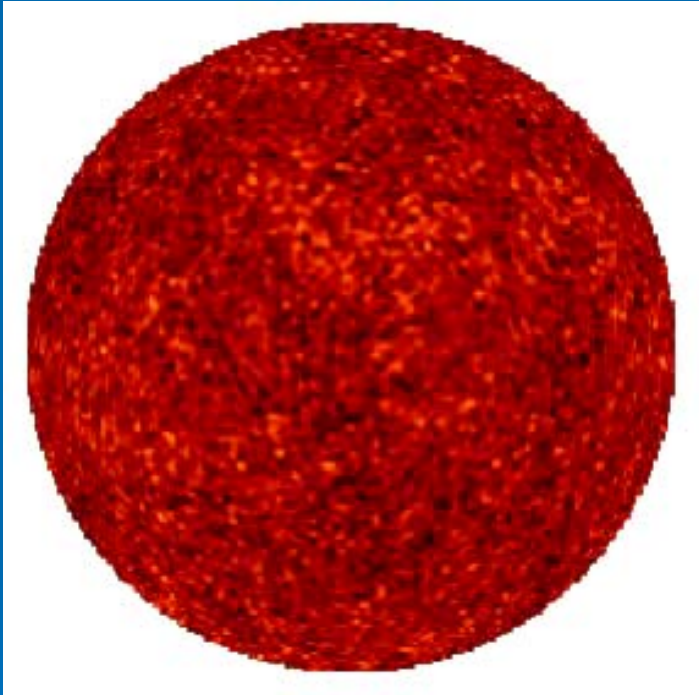


What is the latitudinal structure of the tachocline?
How deep is the return meridional flow?
What are the changes in the tachocline with the solar cycle?

Measurement Schemes: Surface Focusing and Deep Focusing

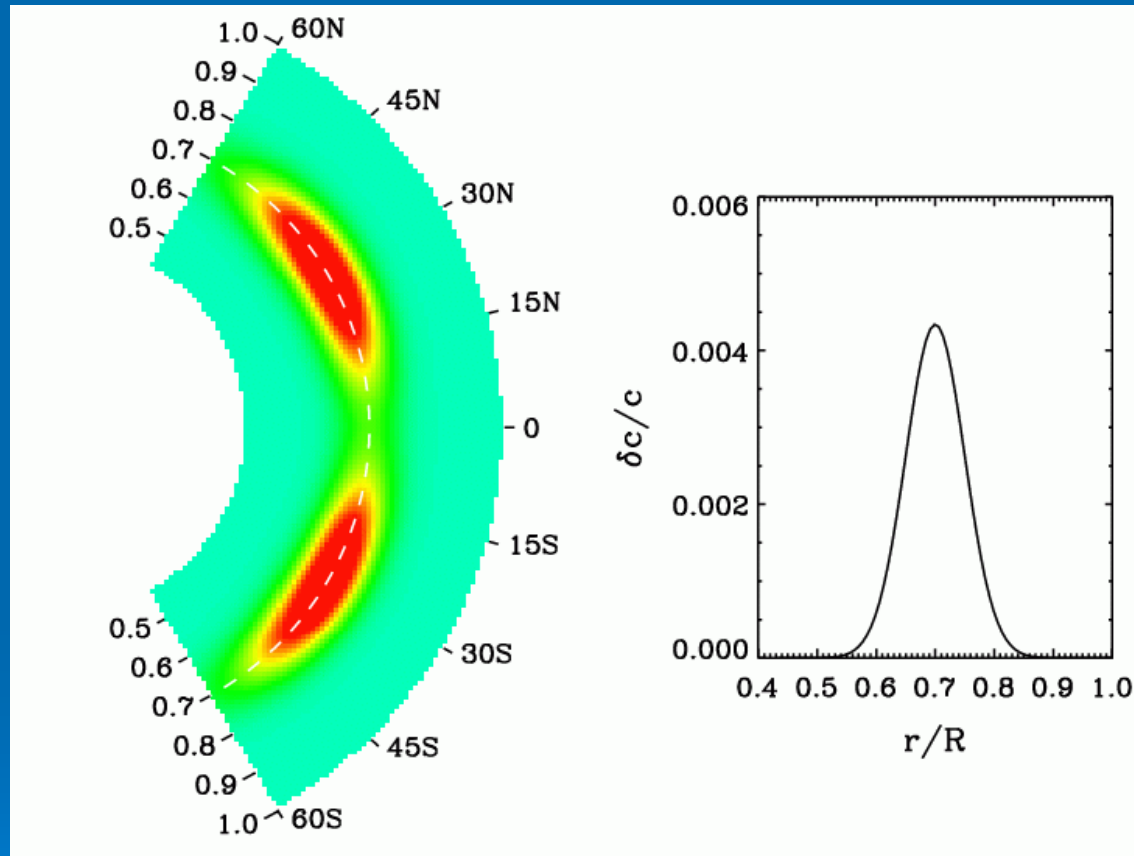


Numerical Simulation of Global Wavefields (by Hartlep & Mansour)



A linear code solving wave propagation equations, including only spherical degree from 0 to 170.

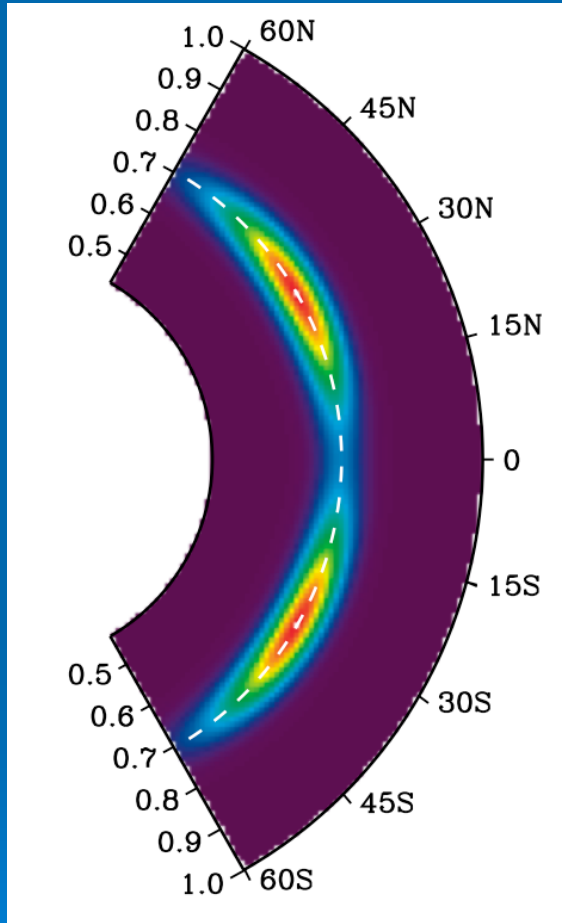
Simulation Model



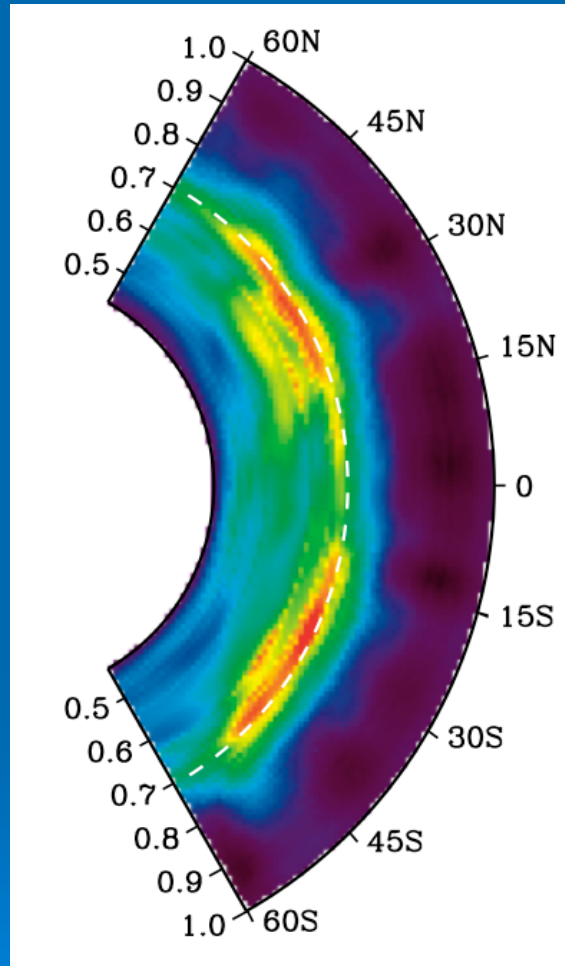
Sound-speed perturbation of 0.6% is placed at $0.7R$, with a latitudinal dependence, and with a Gaussian shape. It's symmetric along the equator.

The simulation used here is 1024 minutes.

Surface Focusing: Comparing Inversion Result with Model



Model



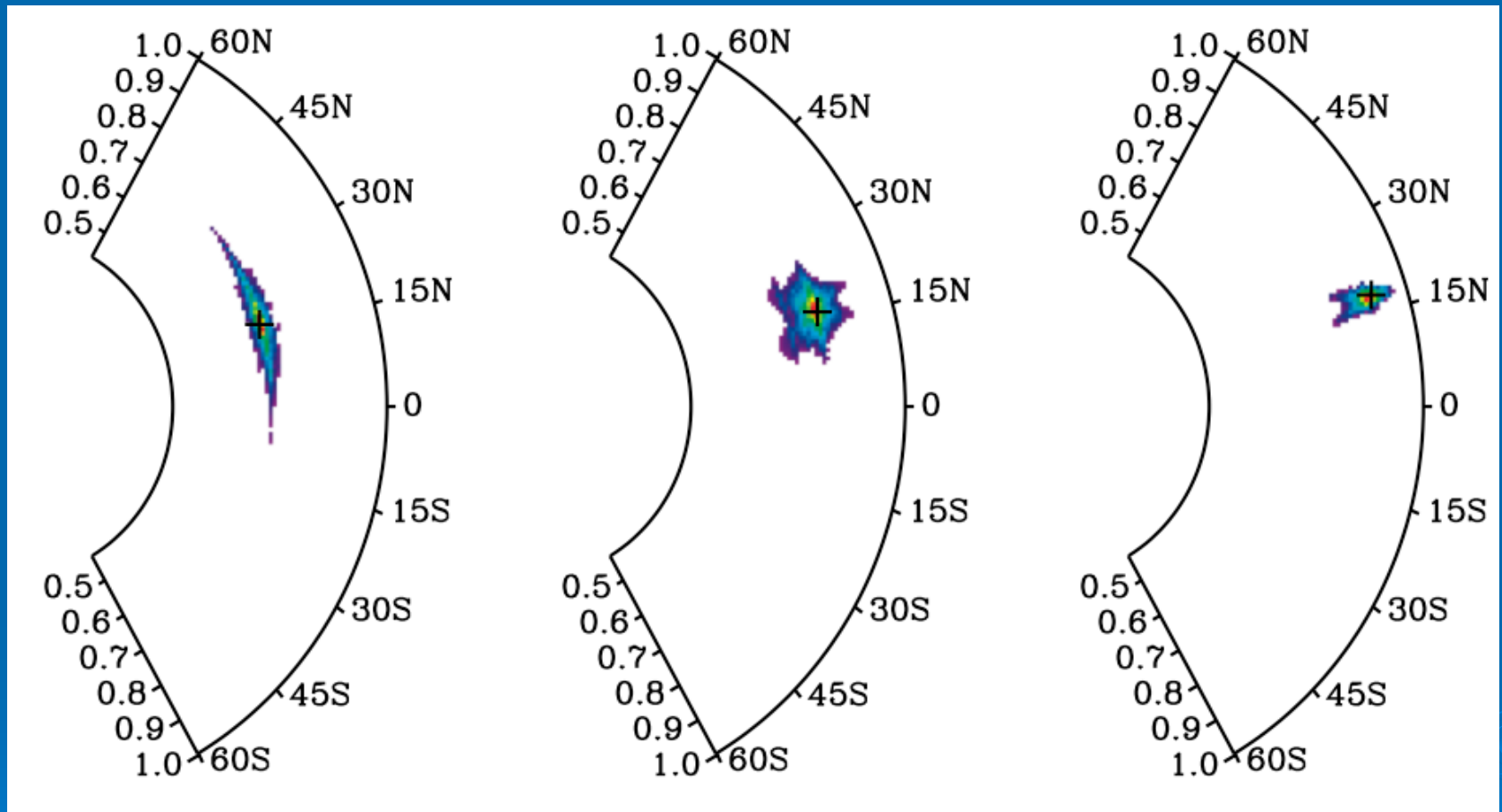
Inversion

The inversion recovers the location of the maximum perturbation well.

The results are more spread out, though, especially towards the deeper interior. (may be related to relatively high realization noise (short time series))

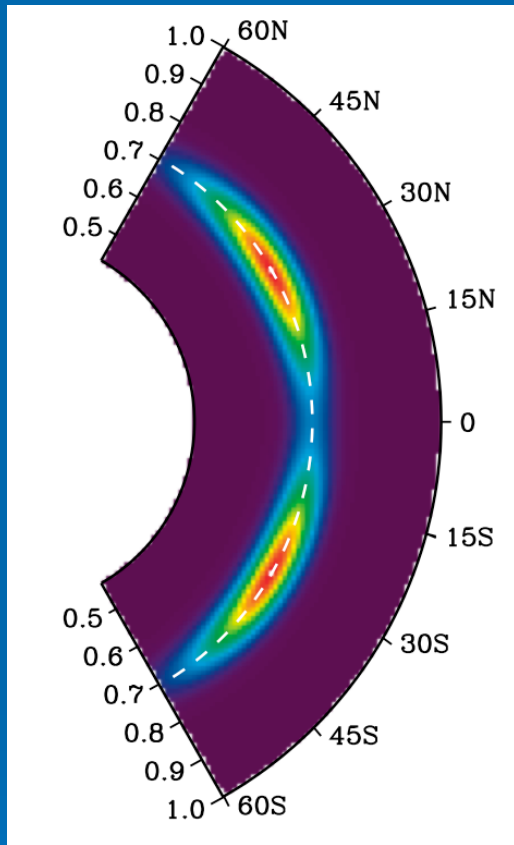
The latitudinal variation is not recovered perfectly, but still promising.

Surface Focusing: Averaging Kernels

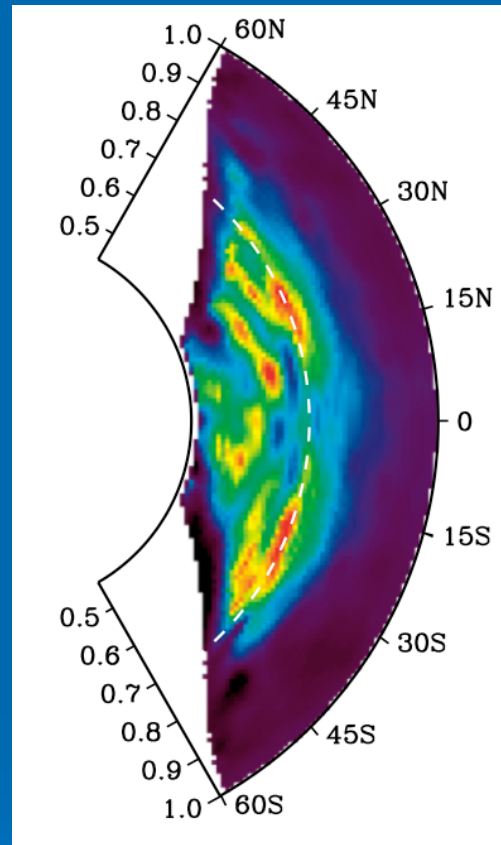


Averaging kernels obtained from surface-focusing inversions when the target location is at a latitude of 18 degree, and at 0.7R, 0.8R, and 0.9R.

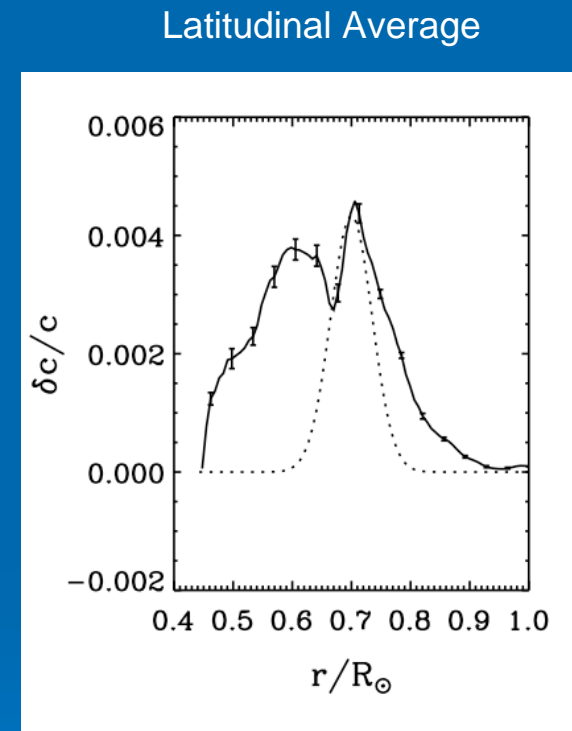
Deep Focusing: Inversion Result



Model

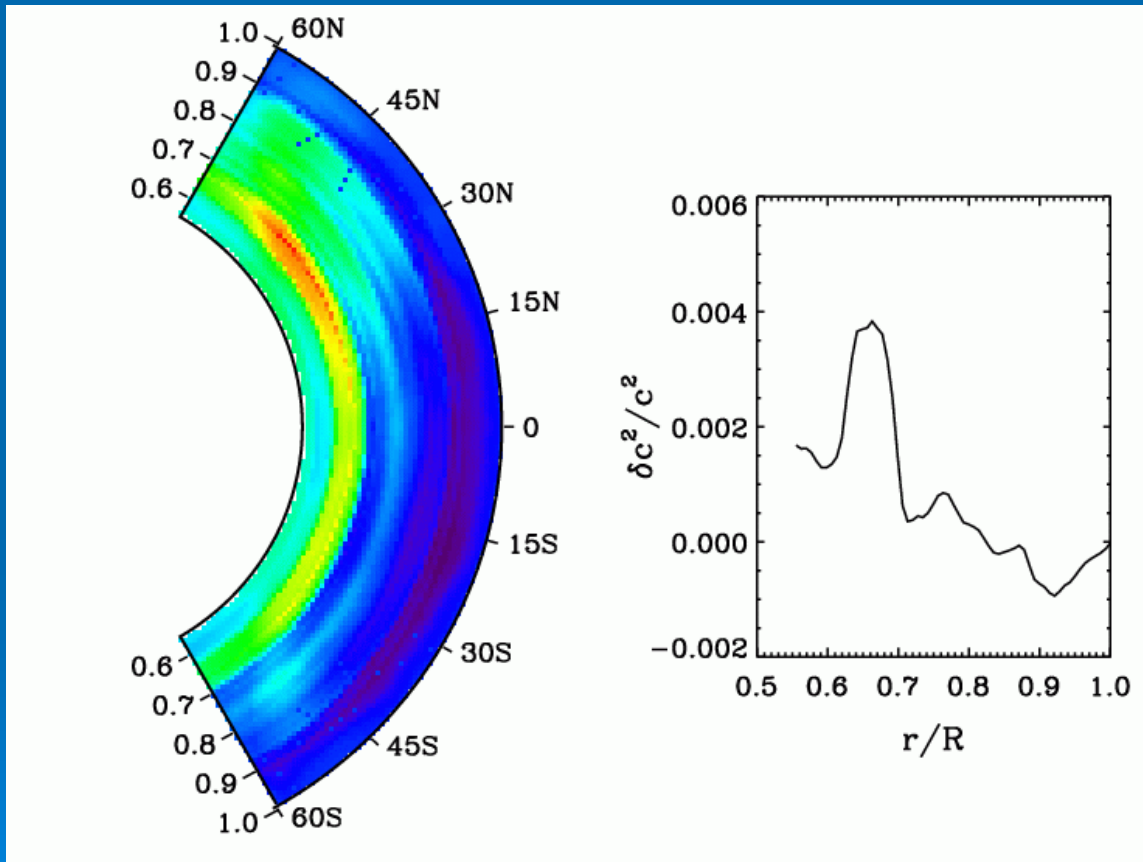


Inversion



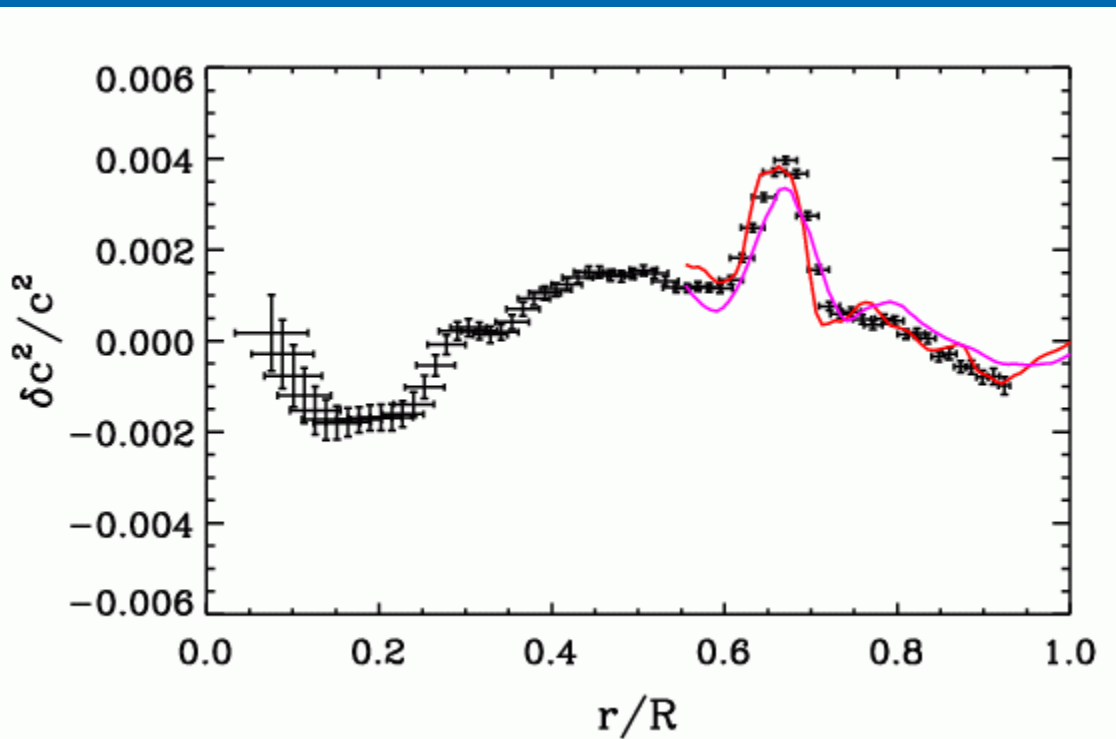
- Results are not quite as good as the surface-focusing results.
- One reason is that measurement noises are high.

Results from Real Sun: Surface Focusing



- Structures are not hemisphere symmetric.
- Tachocline is clearly seen, pretty much latitudinal dependent.

Results: Comparing with Global Helioseismology Result

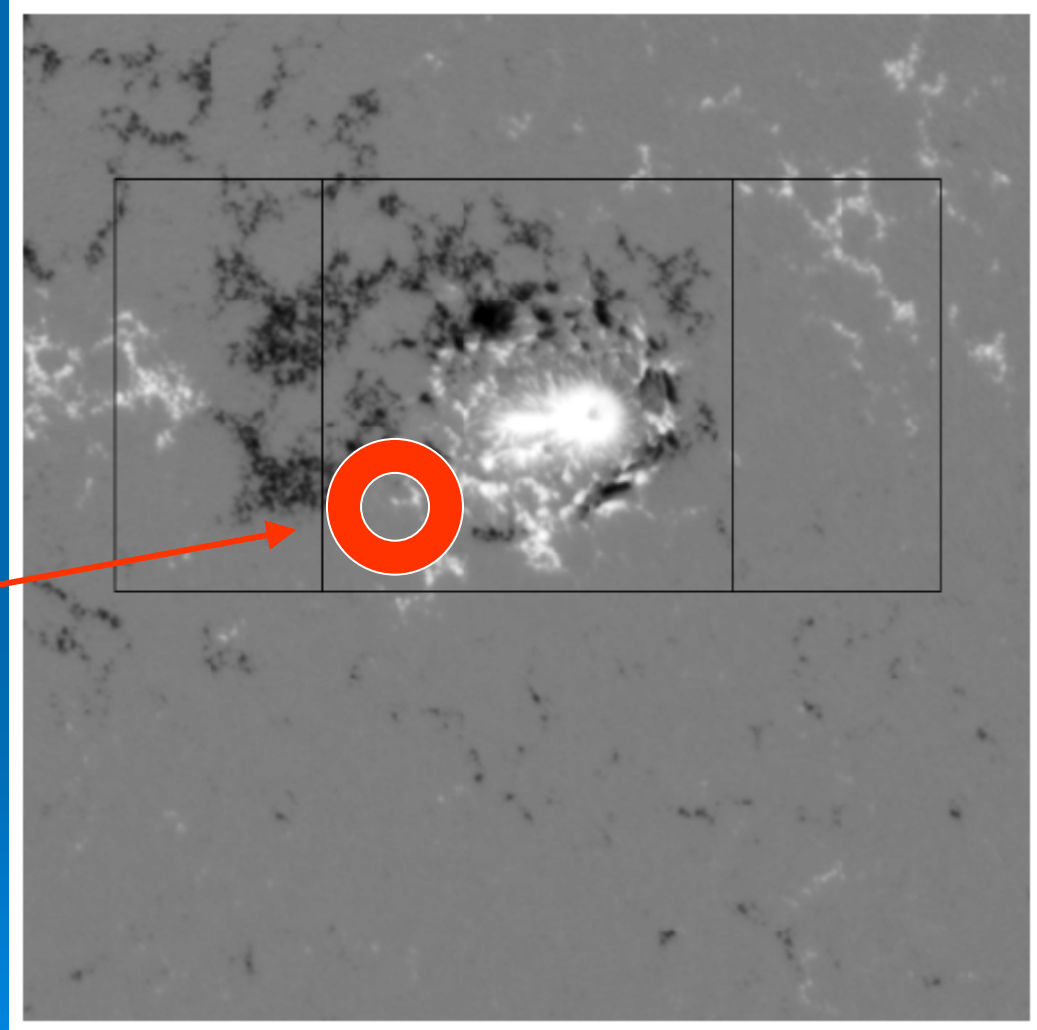


- Red and pink curves are from surface- and deep-focus, respectively.
- Tachocline is surprisingly in good agreement!
- Should keep in mind the experiments using simulated data show that results are not well localized.
- The next step is investigate variations with the solar cycle. This requires careful analysis of MDI instrumental effects.

Hinode helioseismology data are well-suited for probing the upper 6 Mm of the convection zone

This portion of the MDI Hi Res Field is 400x400 arcsec. The rectangle is the FPP Field, 320 x 160 arcsec. The square is the central 160 x 160 arcsec.

**Time-
distance
depth range:
0 – 6 Mm;
temporal
resolution:
8 hours**

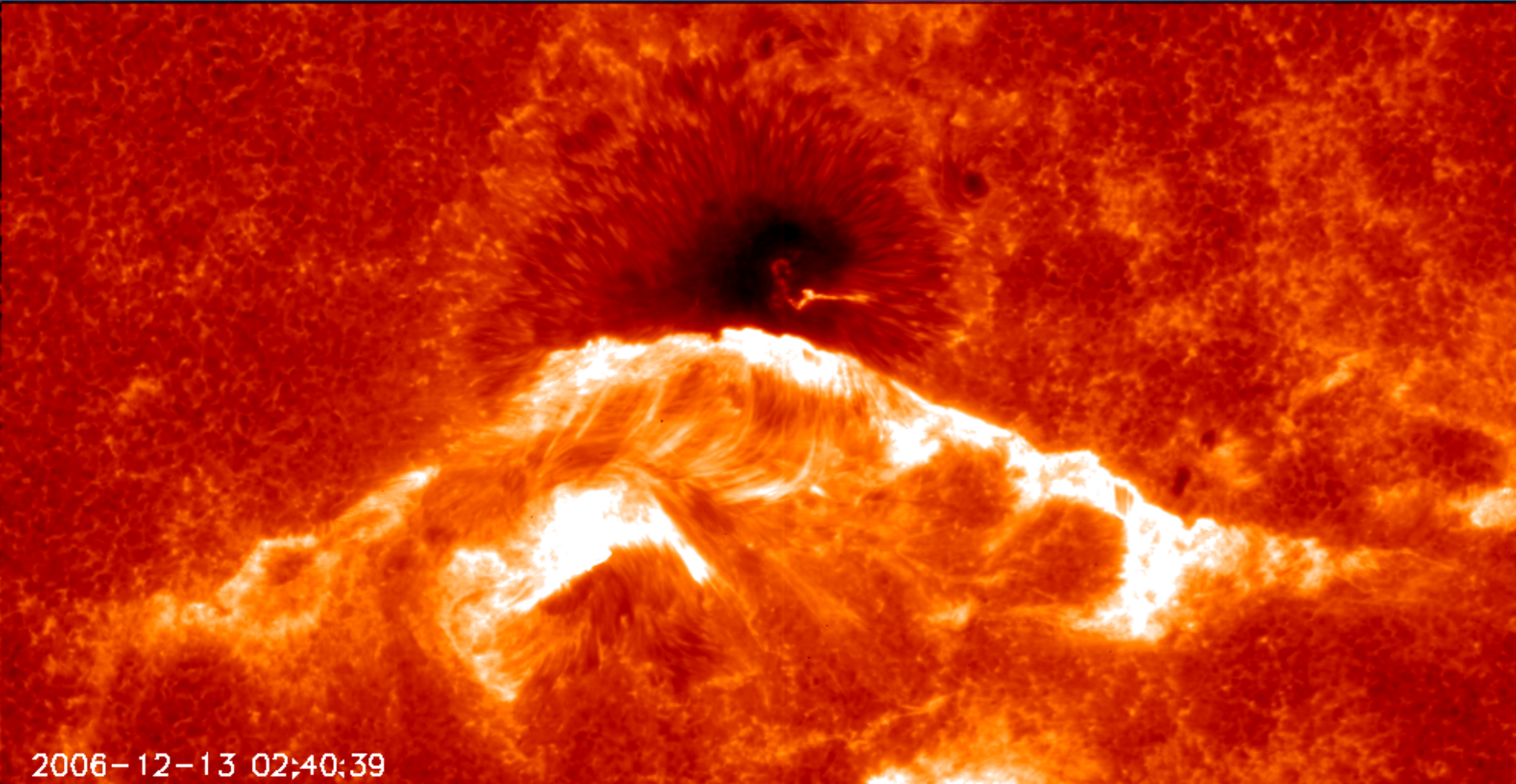


First 5 results of high-resolution helioseismology from Hinode

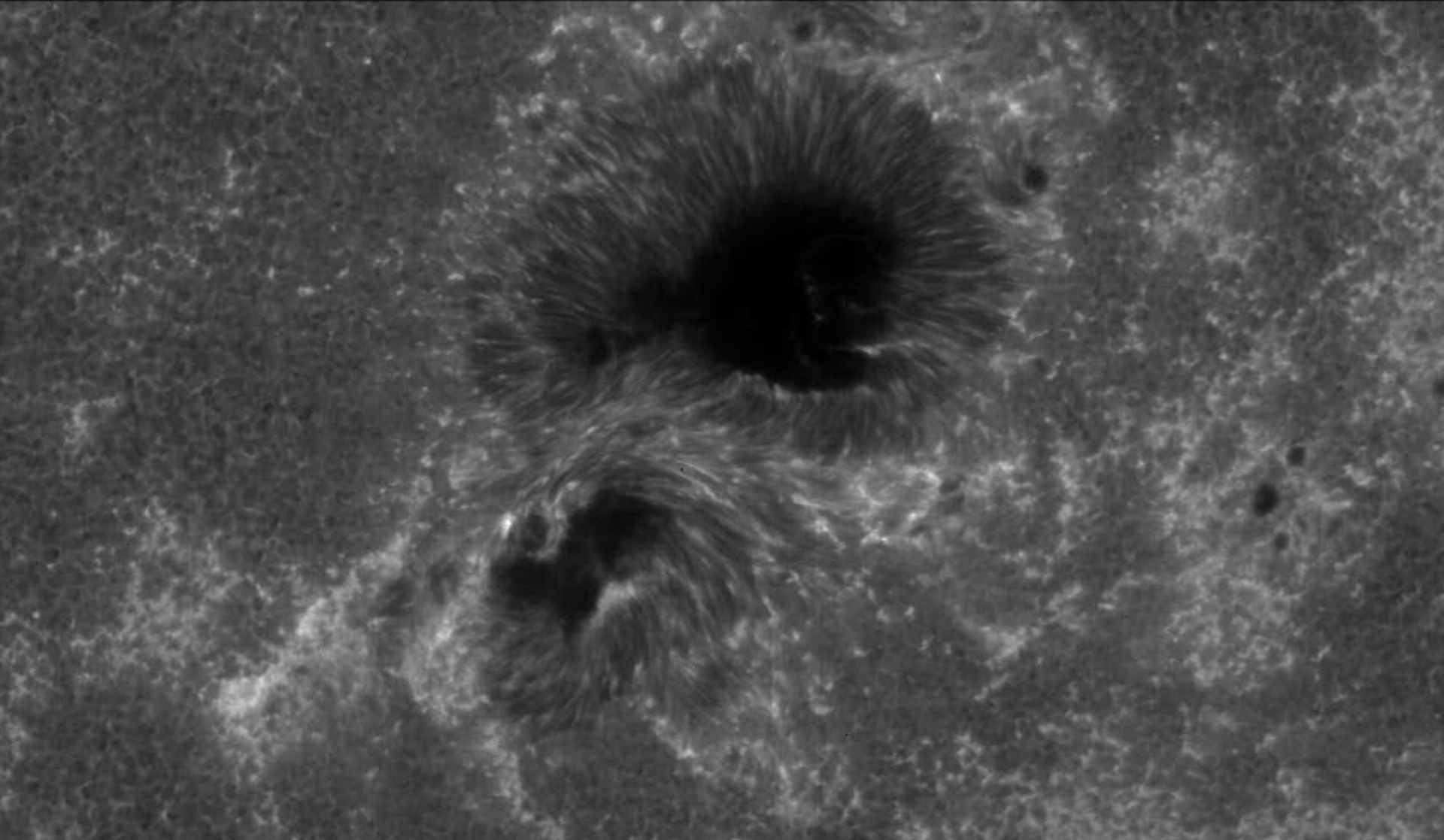
1. **Time-distance helioseismology of supergranular flows in the shallow subphotosphere**
Sekii, Kosovichev, Zhao et al (2007)
2. **Observations of solar oscillations at two heights in the atmosphere**
Mitra-Kraev, et al (2008); Nagashima et al (this session); Fleck et al (poster), Georgobiani et al (poster)
3. **High-resolution oscillation power maps in sunspots**
Nagashima, Sekii, Kosovichev et al. (2007)
4. **Discovery of MHD oscillations excited by a solar flare in sunspot umbra**
Kosovichev & Sekii (2007)
5. **Dynamics of the solar polar regions** (work in progress)

First detection of MHD waves in sunspot umbra, excited by solar flare

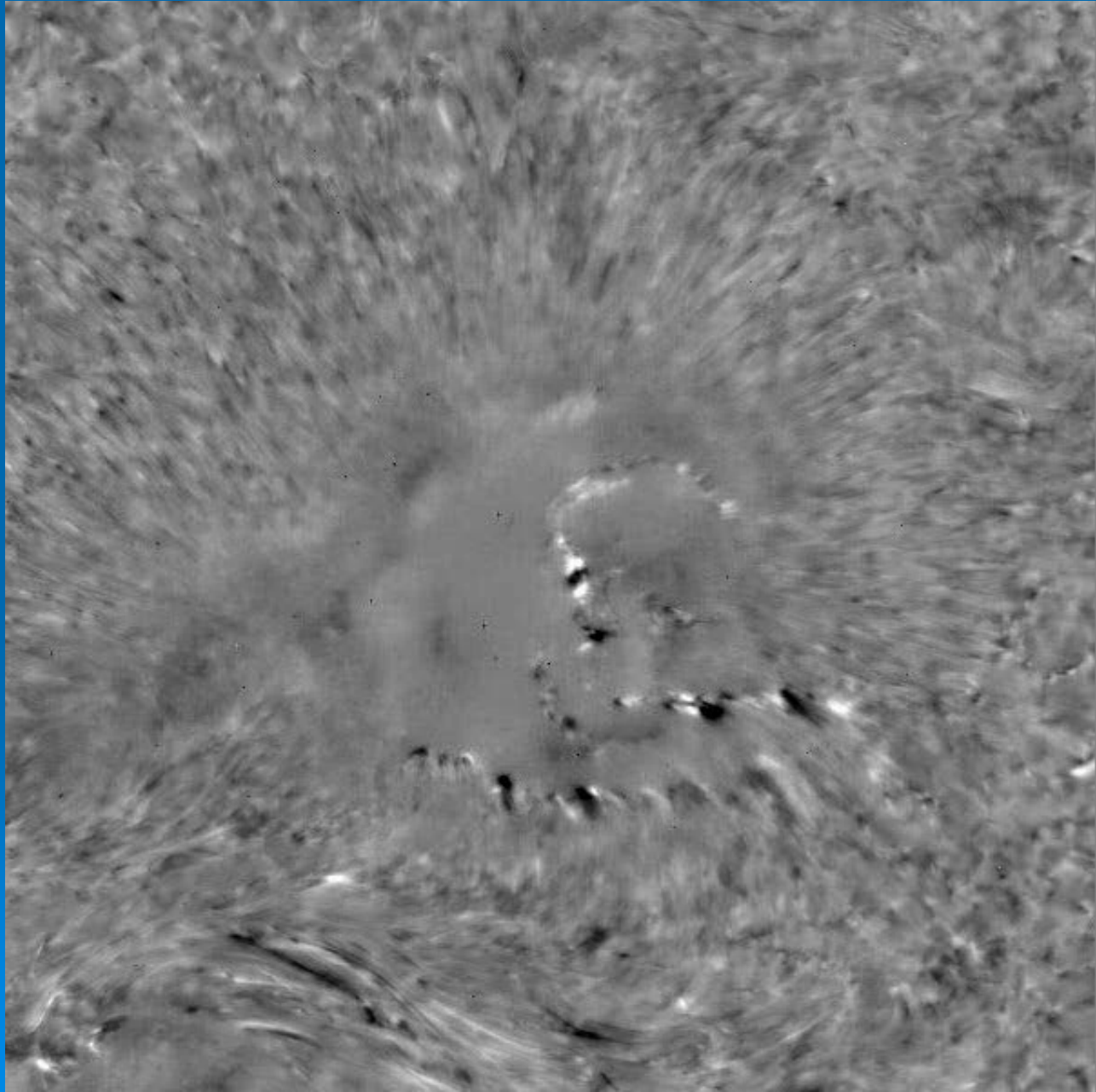
- Hinode/SOT observations of X3.4 flare, December 13, 2006

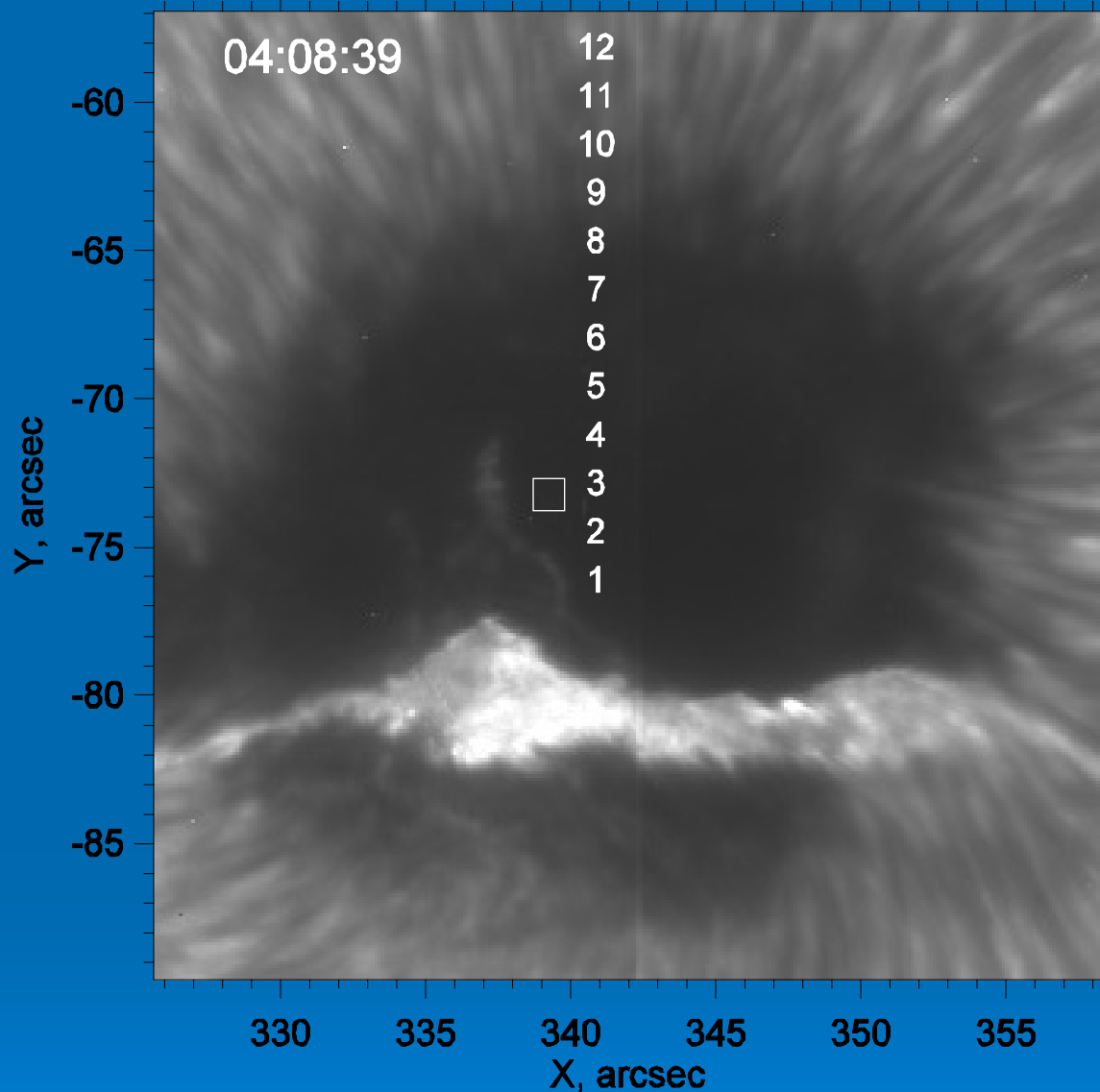


Hinode observations of Dec.13 2006 flare, CaH line



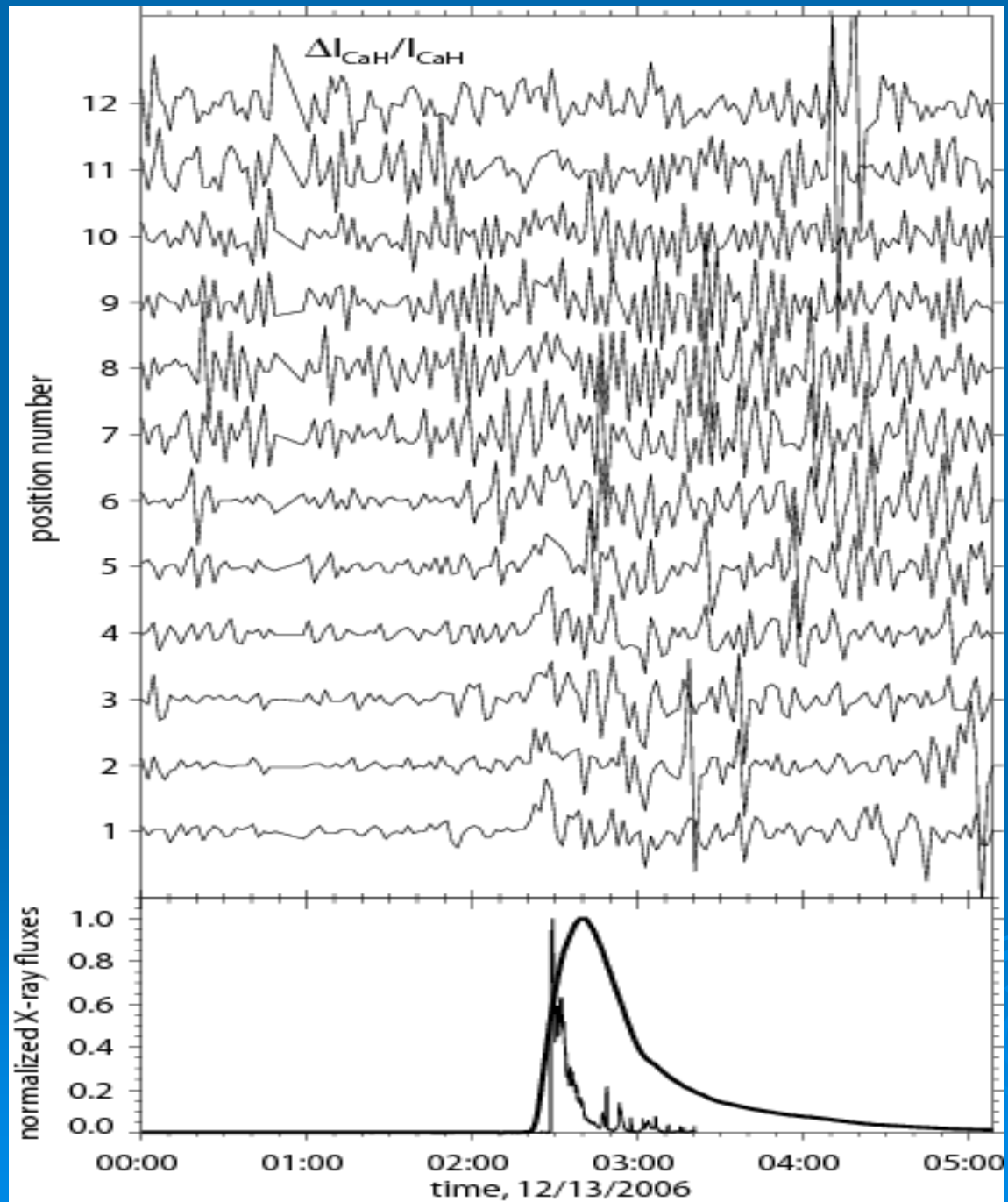
Relative difference movie



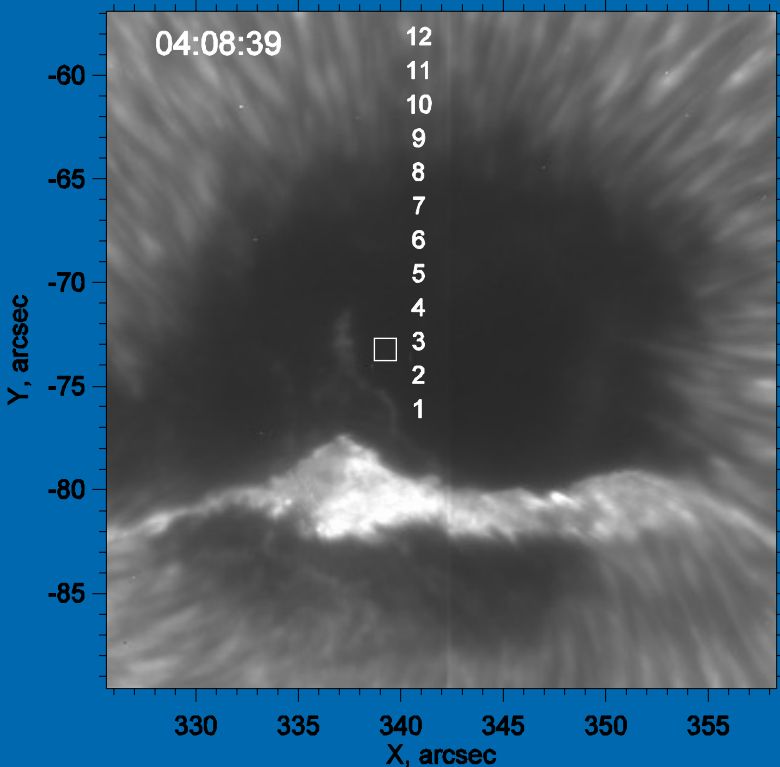


The image of the sunspot umbra with a portion of the flare ribbon at 04:08:39 near the end of the solar flare. The numbers from 1 to 12 show the measurement position. The distance between the points is approximately 1.6 Mm. The small rectangular box is used to study long-term intensity variations.

Relative intensity signals at the selected positions

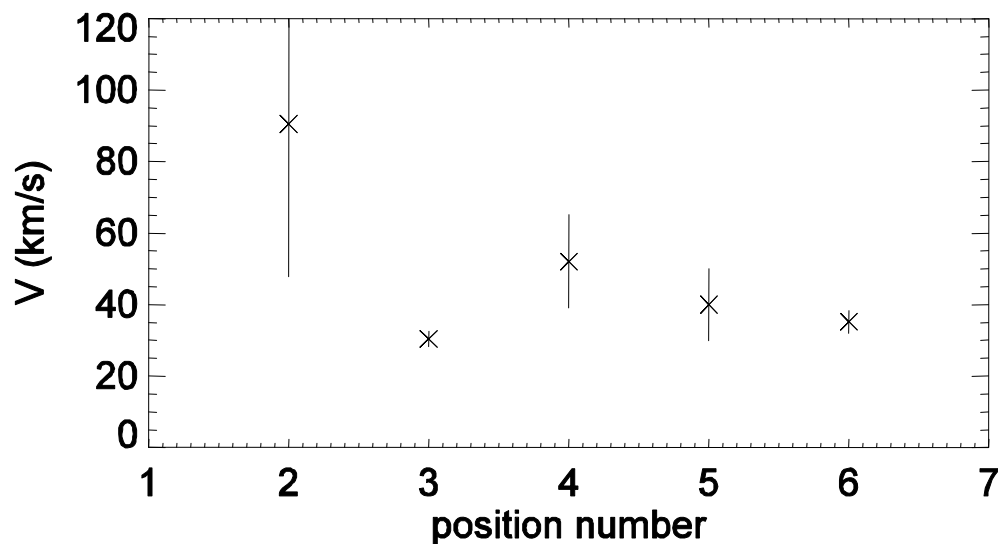
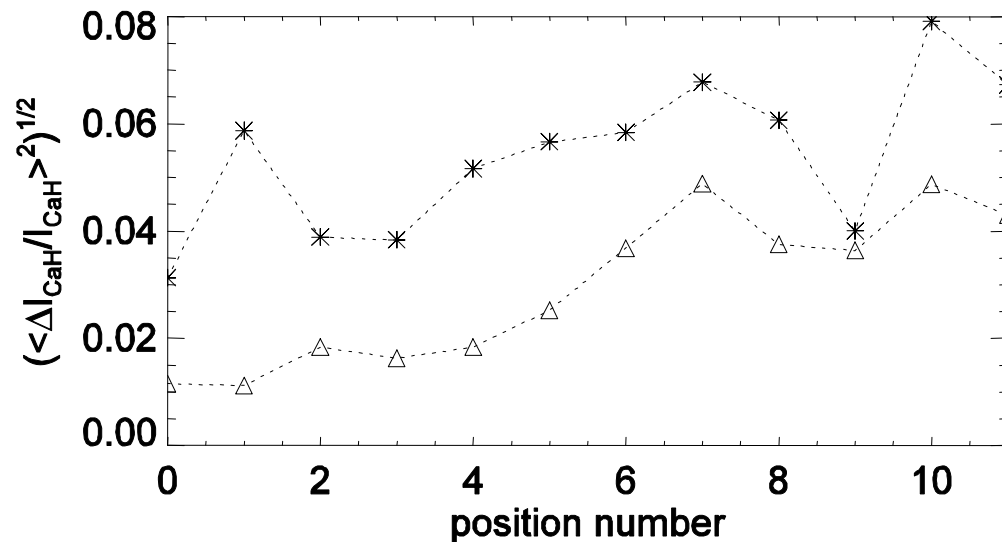


Measurement positions

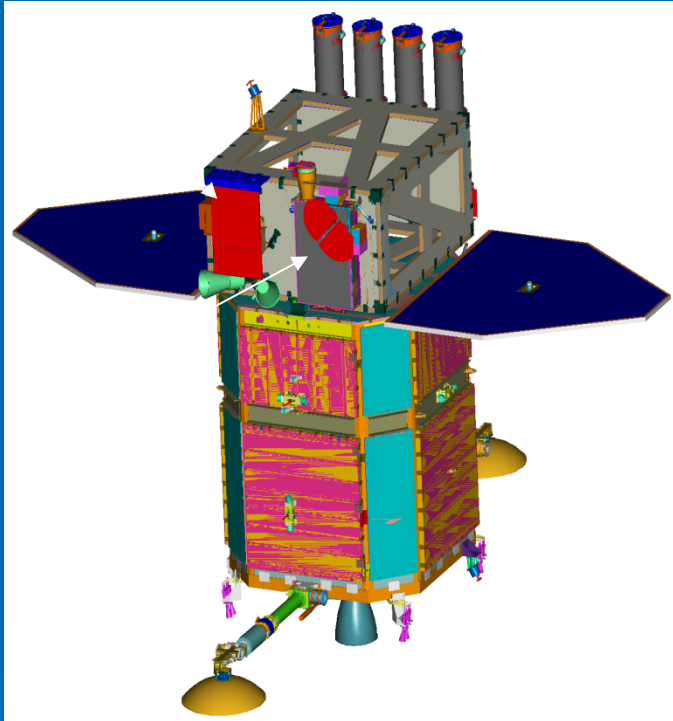


The wave speed is of the order of 50-100 km/s. This is much higher than the sound speed in the chromosphere. Thus, these waves must be of a fast MHD type.
New seismology of sunspots?

Relative RMS oscillation amplitude before the flare (triangles) and after (stars)



SDO - Solar Dynamics Observatory (launch in 2009)



SDO includes:

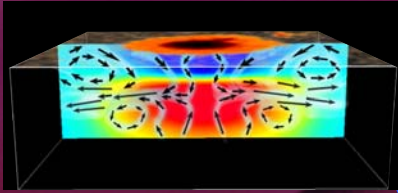
- **AIA** - The Atmospheric Imaging Array
Lockheed Martin Solar and Astrophysics Lab
- **HMI** – Helioseismic and Magnetic Imager
Stanford University with LMSAL
- **EVE** – EUV Variability Experiment
University of Colorado/LASP

SDO will be in an inclined geosynchronous orbit with data collected at White Sands NM and operations managed at GSFC.

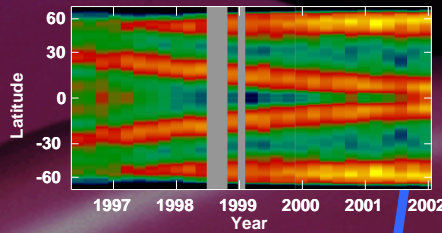
2 TB of data per day

Solar Dynamics Observatory: Helioseismic and Magnetic Imager

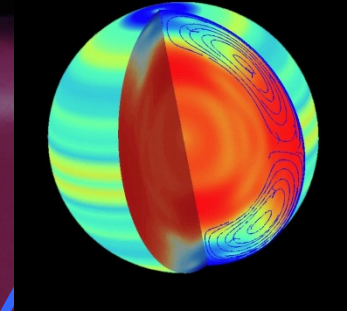
1.J – Sunspot Dynamics



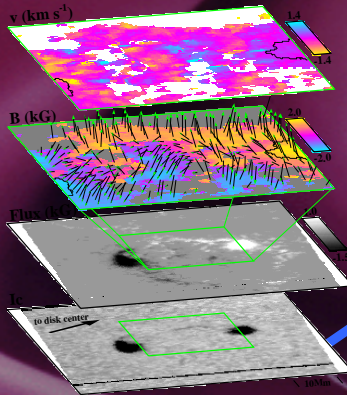
1.B – Solar Dynamo



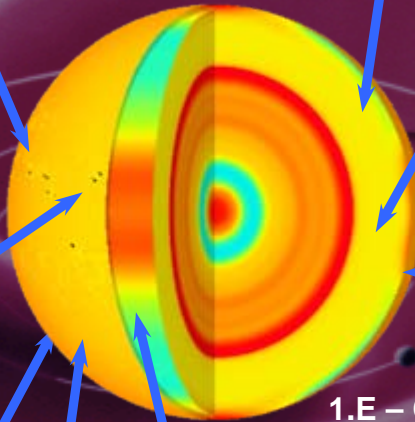
1.C – Global Circulation



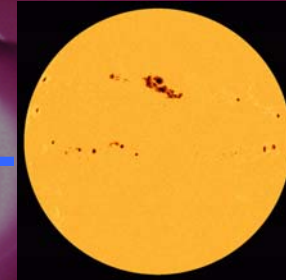
1.I – Magnetic Connectivity



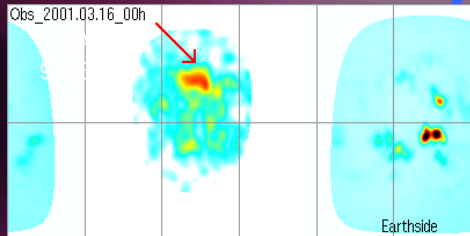
1.A – Interior Structure



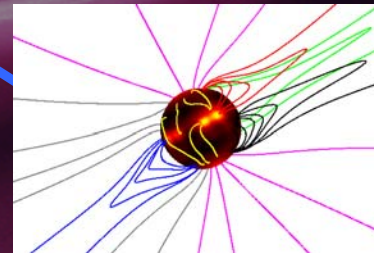
1.D – Irradiance Sources



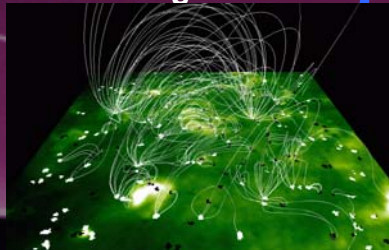
1.H – Far-side Imaging



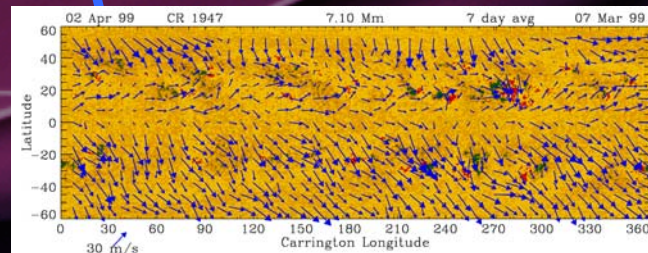
1.E – Coronal Magnetic Field



1.G – Magnetic Stresses



1.F – Solar Subsurface Weather

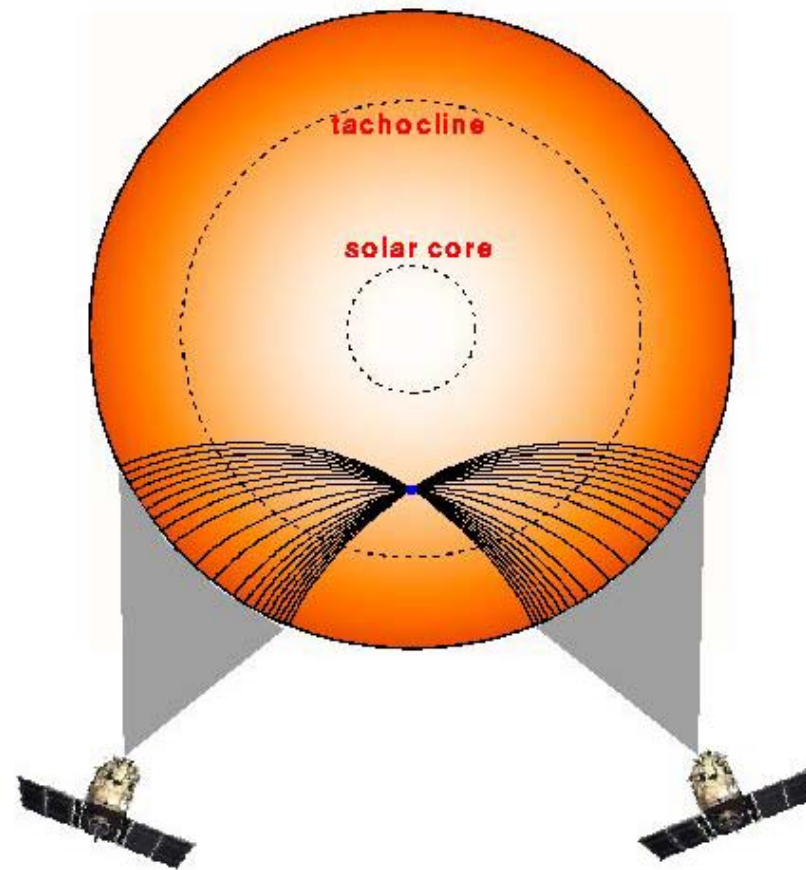


Helioseismology after Hinode and Solar Dynamics Observatory

➤ Main objectives

- Investigation of the polar regions – investigate the mechanism of the Sun's polarity reversals, flux transport and dynamo.
(Solar Orbiter, Solar-C)
- 3D mapping of the whole interior
(Safari)

Stereohelioseismology: time-distance helioseismology of the deep interior (SAFARI mission)



Conclusions

- Helioseismology provides important constraints for dynamo theories of the origin of solar magnetism, new insights into the mechanism of formation of sunspots and active regions.
- It has also demonstrated the importance of subsurface twisting and shearing flows for initiation of solar disturbances, flares and CMEs.
- The future development is based on analysis of high-resolution data from SDO and Hinode, and realistic MHD modeling.